Chapter 2
Low-Temperature Materials Properties

Before delving into the fluids and processes associated with helium cryogenics, it is important to first have a working knowledge of the relevant properties of other materials at low temperatures. This knowledge is valuable in part because materials have behavior that must be taken into account when considering the problems of refrigeration, heat transfer, or storage of low temperature helium. In addition as seen in subsequent chapters, many of the properties of helium are understood in terms of physical models that were primarily developed to treat the properties of different materials at low temperatures.

The study of material properties at low temperatures continues to be an active field of research. Current investigations include studies of the properties of materials at ultralow temperatures, $T \approx 1$ mK, new materials such as alloys and composites as they depend on external variables such as temperature, pressure and magnetic field, and new types of investigation on traditional materials. Much of this work is fundamental in nature. On the other hand, since many material properties play an important role in the design and construction of low-temperature systems, it is essential to have a thorough knowledge of their behavior.

The present chapter is a survey of those properties that are of greatest importance to cryogenic applications. Included in the discussion are the behavior of state properties such as the internal energy and heat capacity, thermal expansion or contraction, transport properties including the electrical and thermal conductivities, and finally mechanical properties. The discussion concentrates on solid elements and alloys. The special properties of superconductors will also be included although the discussion is brief due to space limitations. Most of the descriptions are based on either thermodynamic or solid-state physics principles. More extensive discussions of these topics may be found in textbooks on the relevant subjects [1, 2]. In addition, for applications there are a number of property databases [3, 4] and books [5, 6] that collate available experimental data and can be useful in analysis and design.

S.W. Van Sciver, *Helium Cryogenics*, International Cryogenics Monograph Series,
DOI 10.1007/978-1-4419-9979-5_2,

2.1 Heat Capacity

The heat capacity is a fundamental state property of matter. It represents the amount of energy needed to raise the temperature of a known quantity of a material one degree. The heat capacity per unit mass is called the specific heat. In cryogenic systems, the heat capacity of a material is integral to numerous calculations including: the dynamics of cooling devices from superconducting magnets to sensors, thermal energy storage, dynamic thermal loading on refrigeration systems, and transient heat transfer.

As with many physical properties, the heat capacity is defined in terms of other thermodynamic state variables. In particular, it can be written as a derivative of either the entropy S or internal energy E. Because these state functions are described in a liquid–gas system in terms of an equation of state relating pressure p, temperature T, and specific volume v, one variable usually must be held constant in the definition of the heat capacity or specific heat. For example, the constant volume heat capacity is written in terms of a derivative of the entropy or internal energy as,

$$C_v = T\left(\frac{\partial S}{\partial T}\right)_v = \left(\frac{\partial E}{\partial T}\right)_v \tag{2.1}$$

while the constant pressure heat capacity may be written

$$C_p = T\left(\frac{\partial S}{\partial T}\right)_p = \left(\frac{\partial E}{\partial T}\right)_p + p\left(\frac{\partial v}{\partial T}\right)_p \tag{2.2}$$

It is also possible to define the heat capacity with other external variables held constant. For systems where magnetic properties are of importance, C_H or C_M may be used to designate the heat capacity at constant applied magnetic field or magnetization. This topic is of particular interest in magnetic cooling systems and is discussed in Chap. 10.

A useful relationship between C_p and C_v is obtained from thermodynamic expressions and is given by

$$C_p - C_v = -T\left(\frac{\partial v}{\partial T}\right)_p^2 \left(\frac{\partial p}{\partial v}\right)_T = \frac{Tv\beta^2}{\kappa} \tag{2.3}$$

where $\beta = \frac{1}{v}\left(\frac{\partial v}{\partial T}\right)_p$ is the volume expansivity and $\kappa = -\frac{1}{v}\left(\frac{\partial v}{\partial p}\right)_T$ is the isothermal compressibility.

An extensive amount of experimental data exists for the heat capacity of solids at low-temperatures. For simple solid materials such as metals and crystalline insulators, there is a very good match between experiment and theory. For example, measurements near and above room temperature give close correspondence with

the classical model of harmonic oscillators due to DuLong and Petit for which the heat capacity is equal to $3N_0k_B = 3R$, where N_0 is Avogadro's number = 6.023×10^{23} molecules/mole and k_B is Boltzmann's constant = 1.38×10^{-23} J/molecule K. The gas constant $R = 8.31$ J/mol K. This classical model is based on the equipartition of energy which assigns $\frac{1}{2}k_BT$ to each of the three kinetic energy and three potential energy degrees of freedom in the three-dimensional solid.

At low temperatures, there is markedly different behavior according to the type of solid considered. Over most of the cryogenic range for crystalline solids, the dominant temperature dependence is proportional to T^3. At very low temperatures, $T \lesssim 10$ K, crystalline insulators maintain the T^3-dependence while metals have heat capacities that become linearly proportional to temperature as $T \to 0$. Non-crystalline amorphous materials also have a heat capacity is proportional to T^n where $n \sim 3$. Finally, the difference between C_v and C_p becomes negligible as $T \to 0$ for all solids. This fact can be used in conjunction with (2.3) to show that the volume expansivity, β, must also go to zero at very low temperatures.

2.1.1 Lattice Heat Capacity

Two relatively simple theories are available to describe the general behavior of the heat capacity of metals and crystalline insulators over the entire temperature range of interest [1]. The first such theory is based on the energy contained in the quantized lattice vibrations or phonons that exist in a solid. For most solids, except metals at very low temperatures, this phonon contribution to the heat capacity dominates.

To calculate the phonon heat capacity, we begin with an expression for the internal energy E_{ph} of an ensemble of phonons as a function of their characteristic frequencies ω,

$$E_{ph} = \frac{h}{2\pi}\int D(\omega)n(\omega)\omega d\omega \tag{2.4}$$

In this case, $D(\omega)$, the phonon density of states, describes the fraction of phonons that occupy a particular energy level characterized by its frequency ω. The function $n(\omega)$ is the statistical distribution function, which for phonons obeying Bose-Einstein statistics, is given by [7],

$$n(\omega) = \frac{1}{e^{h\omega/2\pi k_BT} - 1} \tag{2.5}$$

with $h = 6.63 \times 10^{-23}$ J s is Planck's constant. The model-dependent choice in the theory is included in the selection of the proper density of states function, $D(\omega)$. This problem can be quite complicated depending on the detailed nature of the excitations within the solid. Fortunately, many materials at least approximately obey the simplifying assumptions inherent in the Debye model.

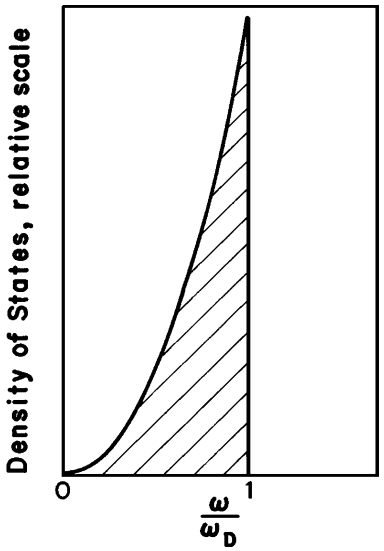

Fig. 2.1 Density of states $D(\omega)$ versus ω for the Debye model for a constant phonon velocity

The Debye model assumes that the density of states is described by a continuum of levels up to the characteristic frequency ω_D, referred to as the Debye frequency. The density of states is then proportional to ω^2 and is shown schematically in Fig. 2.1.

Inserting the Debye density of states and distribution function into the equation for the internal energy of the phonons, (2.4), a nearly closed-form solution for this quantity is obtained,

$$E_{ph} = 9RT\left(\frac{T}{\Theta_D}\right)^3 \int_0^{x_D} \frac{x^3}{e^x - 1} dx \tag{2.6}$$

where $x = h\omega/2\pi k_B T$, $x_D \equiv \Theta_D/T$. The Debye temperature Θ_D is defined in terms of the maximum phonon frequency, ω_D, see Fig. 2.1. The Debye temperature is characteristic to a particular material and has a simple form,

$$\Theta_D = \frac{hc}{2\pi k_B}\left(6\pi^2 \frac{N}{V}\right)^{1/3} \tag{2.7}$$

where c is the speed of sound in the material and N/V is the number of molecules per unit volume. In real materials, the Debye temperature may be a function of more variables than just the number density as described in (2.7), so the above description is only an approximation [1].

The heat capacity in the Debye model can be calculated directly from differentiation of the internal energy, (2.6), with respect to temperature

$$C_{ph} = 9R\left(\frac{T}{\Theta_D}\right)^3 \int_0^{x_D} \frac{x^4 e^x}{(e^x - 1)^2} dx \tag{2.8}$$

The definite integration within (2.8) can be easily performed numerically once Θ_D is known. However, one can obtain considerable insight be studying the limiting form of C_{ph}, which can be checked by evaluating (2.8) at either high or low temperatures relative to Θ_D.

In the high temperature limit, $x_D \ll 1$, the exponentials within the integral may be expanded as $e^x \sim 1 + x$ and simply integrated leading to a constant value for C_{ph}

$$C_{ph} = 3R \; for \; T \gg \Theta_D \tag{2.9}$$

which is the classical Dulong-Petit limit. Note that the heat capacity per mole is constant in this range and on the order of 25 J/mole K. On the other hand, at low temperatures, $x_D \gg 1$, the upper limit of the integral may be taken to be infinite, which makes the exponential terms dominant. The result leads to constant value for the definite integral and a cubic temperature dependence for the heat capacity,

$$C_{ph} = \frac{12\pi^4}{5} R \left(\frac{T}{\Theta_D} \right)^3 \text{for } T \ll \Theta_D \tag{2.10}$$

which accurately reproduces the cubic temperature dependence of the heat capacity observed for many materials at low temperatures. Thus, a measurement of the heat capacity of a solid at low temperature is one way of determining the Debye temperature. Note that (2.10) indicates that low Debye temperature materials will have relatively larger heat capacities at low temperature, which is technically significant for refrigeration.

The simplicity of the Debye model and the dominance of the phonon contribution to the heat capacity over most of the relevant temperature range makes it a useful tool for approximate calculations in cryogenics. One can simply tabulate the C_{ph} and E_{ph}/T in terms of T/Θ_D as is shown graphically in Fig. 2.2. These are universal forms for the Debye phonon heat capacity and internal energy in Joules/mole K that depend only on the value of Θ_D. For most solid materials, the Debye temperatures range from 100 to 1,000 K with examples listed in Table 2.1. This simple analysis is usually accurate to within 20%.

Example 2.1

Using the Debye model, Fig. 2.2, estimate the change in internal energy of a 1 kg copper block when it is cooled from 300 to 80 K.

Molar weight of copper is 0.0635 kg/mol. Thus, 1 kg = 15.75 mol.
The Debye temperature of copper is 343 K (see Table 2.1).
At 300 K, $T/\Theta_D = 0.87$ and at 80 K, $T/\Theta_D = 0.23$

From the graph, E_{ph}/T (300 K) ~ 15 J/mol K; and E_{ph}/T (80 K) ~ 6 J/mol K
Thus, the internal energy is dominated by its 300 K value. For the 1 kg copper block,

$E_{ph} \sim [15 \text{ J/mol K} \times 300 \text{ K} + 6 \text{ J/mol K} \times 80 \text{ K}] \times 15.75 \text{ mol} = 63 \text{ kJ}$.

Note: This problem could also be solved numerically by integration of (2.8).

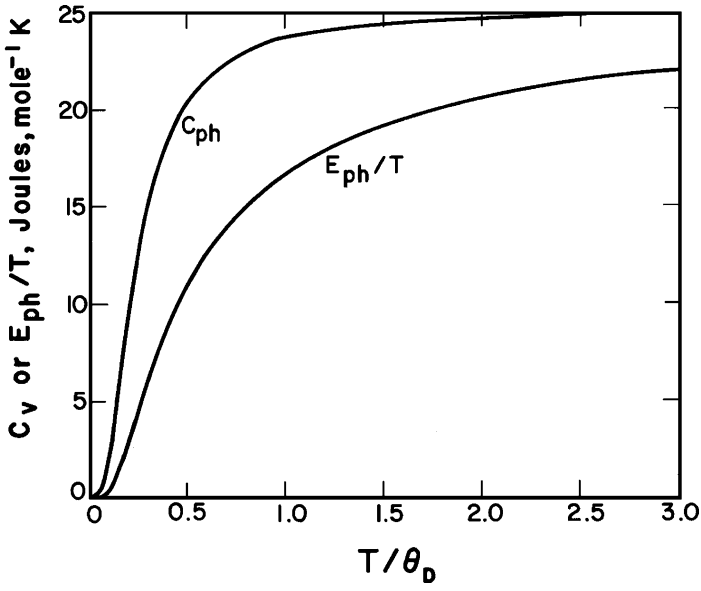

Fig. 2.2 Debye specific heat and internal energy functions

Table 2.1 Debye temperatures for common elements in cryogenics [1]

Element	Θ_D (K)
Al	428
Au	165
Cd	209
Cr	630
Cu	343
Fe	470
Ga	320
Hf	252
Hg	71.9
In	108
Nb	275
Ni	450
Pb	105
Sn	200
Ti	420
V	380
Zn	327

2.1.2 Electronic Heat Capacity

For metals at low temperatures, $T < 10$ K, there is an additional significant contribution to the heat capacity due to the energy contained in the conduction electrons. Fortunately, as with the phonon contribution, the electron contribution to the heat capacity can also be approximately described by a simple theory. The free-electron model treats the conduction electrons as a non-interacting gas of spin ½ particles. Thus, as in the case of the Debye model, the internal energy of the electron gas E_e is written in terms of the density of states $D(\varepsilon)$ [1],

$$E_e = \int D(\varepsilon) f(\varepsilon) \varepsilon d\varepsilon \tag{2.11}$$

where ε is the electron energy used as a variable in this case instead of frequency in the Debye model. The density of states in the free-electron model is written,

$$D(\varepsilon) = \frac{V}{2\pi^2}\left(\frac{m}{2\pi^2}\right)^{3/2} \varepsilon^{1/2} \tag{2.12}$$

Since electrons are spin ½, they must obey Fermi-Dirac statistics, which means that each energy level can have no more than one electron. The Fermi – Dirac distribution function is [7],

$$f(\varepsilon) = \frac{1}{e^{(\varepsilon-\mu)/k_B T} + 1} \tag{2.13}$$

where μ is the chemical potential, which is approximately equal to the Fermi energy, ε_f, at low temperatures [1].

The free-electron model defines the Fermi energy ε_f in terms of the total number of free electrons per unit volume, N_e/V

$$\varepsilon_f = \frac{h^2}{8\pi^2 m_e}\left(3\pi^2 \frac{N_e}{V}\right)^{2/3} \tag{2.14}$$

where m_e is the mass of an electron equal to 9.11×10^{-31} kg. Thus, the Fermi energy only depends on the number density of electrons. One can also define a characteristic temperature, called the Fermi temperature, $T_F = \varepsilon_F/k_B \sim 10^4$ K.

Ordinarily and certainly in cryogenics, the electron temperature in a metal is far below the Fermi temperature so that only a small fraction of the electrons near the Fermi surface contribute to the thermal properties. Because $T \ll T_F$, the electrons in a metal generally are referred to as a degenerate Fermi gas. For a degenerate Fermi gas the internal energy (2.11) can be simply evaluated. The electronic contribution to the heat capacity then turns out to be linearly proportional to the absolute temperature,

$$C_e = \gamma T \tag{2.15}$$

Table 2.2 Coefficient of the electronic specific heat for various metallic elements of technical interest [1]

Element	γ(mJ/mol K^2)
Ag	0.646
Al	1.35
Au	0.729
Cr	1.40
Cu	0.695
Fe	4.98
Ga	0.596
Hg	1.79
In	1.69
Nb	7.79
Ni	7.02
Pb	2.98
Sn	1.78
Ti	3.35
V	9.26
Zn	0.64

where $\gamma = \frac{1}{3}\pi^2 D(\varepsilon_F)k_B^2$ is sometimes called the Sommerfeld constant with $D(\varepsilon_F)$ being the electron density of states evaluated at the Fermi energy (2.14). The Sommerfeld constant has been measured for many metals and some typical values are listed in Table 2.2. To give a rough idea of the importance of the electronic contribution to heat capacity, one should note that for copper the electron and phonon contributions are equal at about 3.8 K.

2.1.3 Heat Capacity of Special Materials

The above general trends in the heat capacity of solid materials are fairly universal. However, they do not describe all materials and the usefulness of the Debye and free electron models is limited. In other cases, the knowledge of the heat capacity of materials is more empirical.

Figure 2.3 is a plot of the specific heat of a variety of materials used in cryogenics [6]. Note that these materials display similar trends in C_p to the theory discussed above. The pure metals (Fe, Cu, Al, Be) show a linear dependence at low temperatures ($T < 10$ K) followed by a transition region where C_p is proportional to T^3 and finally appproach a near constant value above 100 K. The metallic alloys (stainless steel, brass) generally do not display the linear region due to a smaller contribution by free electrons otherwise their behavior is similar to that of pure metals. Non-metals (Pyrex, glass resin) show only a T^n dependence ($n \sim 3$) at low temperatures due to the dominance of the phonon excitations.

Also, there are certain special materials that have anomalous low temperature heat capacities that are unique and also significant for cryogenic applications.

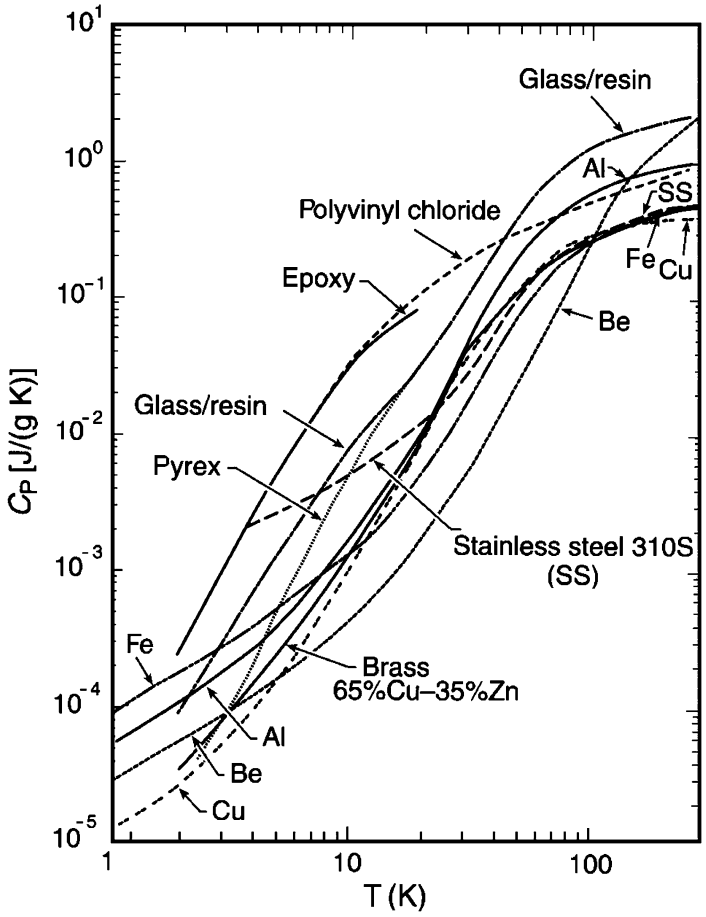

Fig. 2.3 Specific heat capacity of technical materials used in cryogenics (Reprinted from Ekin [6])

One such class of materials are those that undergo magnetic ordering transitions at low temperatures. These transitions produce a large peak in the specific heat, see Fig. 2.4. Most of these materials consist of rare earth compounds where the magnetic ions such as gadolinium (Gd^{++}) undergo ordering at low temperatures. These materials are useful as thermal capacity stores in low temperature cryocooler regenerators, a topic discussed in that context in Chap. 8. They are also used in magnetic refrigeration where the order – disorder transition can be driven by application of a magnetic field. This topic is discussed in Chap. 10.

Finally, superconducting materials undergo phase transitions with a discontinuity in the heat capacity at the onset of the superconducting state, $T = T_c$. Below T_c, the heat capacity of a superconductor decreases rapidly below that of the normal state, particularly at very low temperatures where the phonon contribution is small.

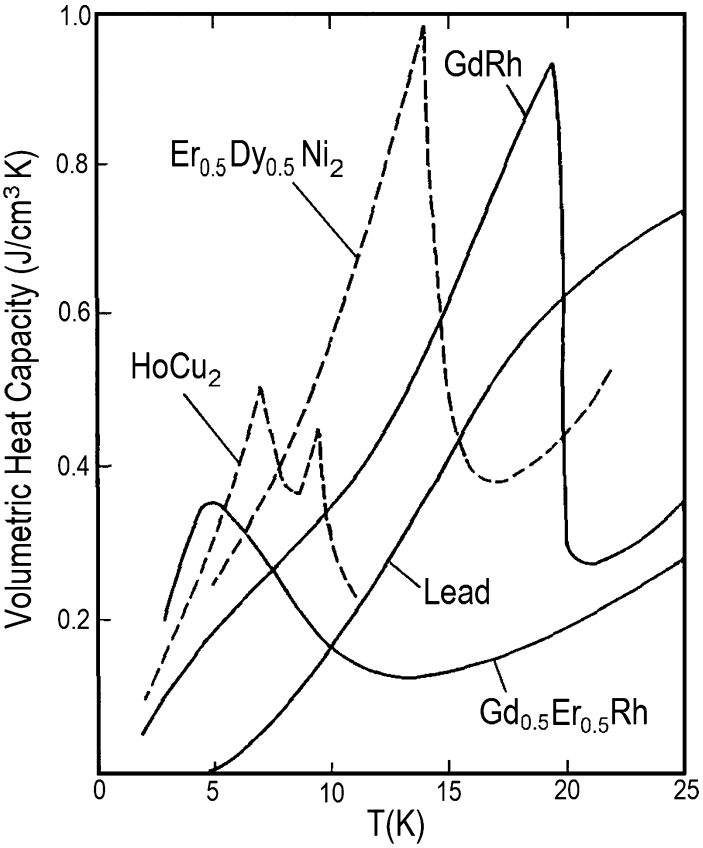

Fig. 2.4 Volumetric specific heat to metallic compounds with low temperature phase transitions (Reprinted from Nageo, et al [8])

This behavior has to do with the very nature of superconductivity, a topic that is discussed further in Sect. 2.5.

2.2 Thermal Contraction

All materials experience a change in physical dimension when cooled to low temperatures. This effect, normally referred to as thermal contraction in the field of cryogenics, is typically on the order of a few tenths of a percent change in volume in most materials between room temperature and liquid helium temperatures. Although the effect is not large in absolute magnitude, it can have a profound impact on the design of engineering devices operating in a low-temperature environment. The thermal contraction coefficients of different materials vary by as much as an order of magnitude. Furthermore, since most devices constructed to

operate in cryogenic systems are fabricated at room temperature out of a number of different materials, one of the major concerns is the effect of the differential thermal contraction and the associated thermal stress that may occur when two dissimilar materials are bonded together. Differential contraction is especially important to the design of low temperature vacuum seals, structural supports, and electrical insulation systems. Thus, it is of considerable importance to understand this behavior of technical materials. There are a number of good reviews in the literature on this subject [9–12].

The thermal contraction or expansion has a thermodynamic definition, which can be combined with other state properties to make predictions of the details of the properties of materials at low temperatures. For liquids and gases, the most meaningful form to consider is the volume expansivity defined as,

$$\beta = \frac{1}{V}\left(\frac{\partial V}{\partial T}\right)_p \tag{2.16}$$

where β is in general a function of temperature. For solids, where the changes in individual dimensions may be different due to anisotropic effects, the linear thermal expansion coefficient,

$$\alpha = \frac{1}{L}\left(\frac{\partial L}{\partial T}\right)_p \tag{2.17}$$

is a more appropriate and common factor to consider and is the value that is tabulated in the literature. For isotropic materials, $\alpha = 1/3\beta$ to first order. For many common solids near room temperature, the linear expansion coefficient is approximately constant.

In a solid, the thermal expansion is caused by anharmonic terms in the restoring potential between the individual molecules. Recall that the Debye model assumes that a solid is comprised of a set of harmonic oscillators. Therefore, the Debye model in its simplest form does not predict the existence of thermal expansion. Anharmonic terms in the interaction potential are what cause the non-zero β. For molecules in a solid, the anharmonic terms can be represented as variations in the Debye temperature Θ_D with the specific volume. This variation may be written,

$$\gamma_G \equiv -\frac{d(\ln \Theta_D)}{d(\ln V)} \tag{2.18}$$

where γ_G is referred to as the Grüneisen coefficient, values of which for a few elements are listed in Table 2.3. The Grüneisen coefficient, which is nearly constant over a temperature range down to $T \approx \Theta_D/5$, can be used along with other thermodynamic properties to calculate the thermal expansion coefficient,

$$\alpha = \frac{\gamma_G C_v \kappa}{3v} \tag{2.19}$$

Table 2.3 Values for the Grüneisen coefficient y_G for common elements [1]

Element	y_G
Ag	2.40
Al	2.17
Cu	1.96
Fe	1.6
Ni	1.88
Pt	2.54

where κ is the isothermal compressibility. For metals at low temperatures, $T < \Theta_D/25$, the dominant temperature dependence of α is in the specific heat, $C_v \approx \gamma T + \beta T^3$.

At low temperatures, the expansion coefficient is far from linear and actually approaches absolute zero with zero slope, a fact that can be understood in terms of thermodynamics. In (2.3), the difference between the constant volume and constant pressure heat capacity is shown to be proportional to the square of the volume expansivity β. Since according to the Third Law of Thermodynamics, the quantity $(C_p - C_v)$ must go to zero as $T \rightarrow 0$, it follows that β also must do so. This effect makes sense physically because the harmonic terms would be expected to dominate the interatomic potential at such low temperatures.

Because of the nonlinear nature of α and β, it is often more useful to have the integrated thermal contraction for the purpose of design. Figure 2.5 displays the integrated linear contraction of a number of common materials used in cryogenic applications [6]. Note that metals typically have total contractions in the range of 0.5% or less with the lowest value being for Invar, which is a special metal designed to have a low value of α. Polymers such as epoxy or Teflon contract about three times as much as metals and can have a total contraction between 300 and 4 K as high as 2%. Some amorphous materials, particularly Pyrex, have nearly zero or sometimes negative thermal contraction coefficients.

Composite materials often can have their thermal contraction predicted based on a linear combination of the two individual materials, taking into account the elastic modulus of each constituent. This approach to estimating the thermal contraction of a composite is referred to as the rule of mixtures. However, composite materials are frequently anisotropic by design, which makes their linear contraction coefficients dependent on the internal structure and orientation of the component materials. A clear example of this behavior can be seen in the structural material, G-10, which is a composite of epoxy and fiberglass. In this case, the thermal contraction of the composite depends on the volume ratios of the two materials and the orientation of the fibers within the composite. For example, the integrated $\Delta L/L$ from 300 to 4.2 K is about 0.25% for G-10 in the fiber direction (wrap) and about 0.75% normal to the fiber direction.

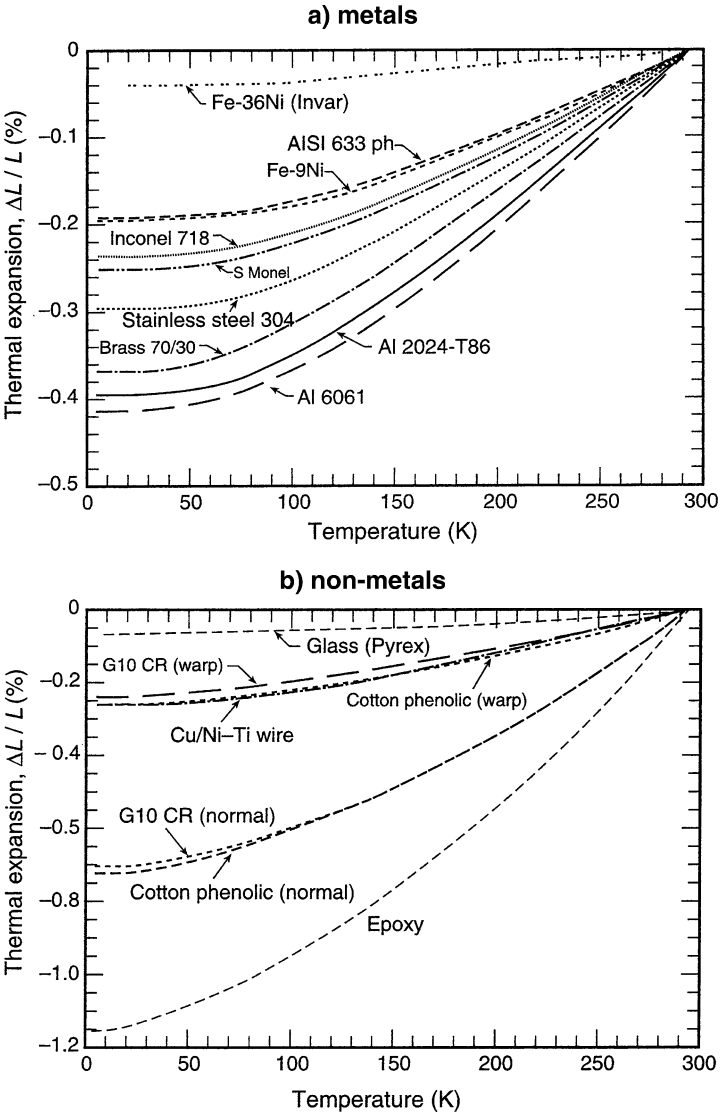

Fig. 2.5 Total thermal expansion/contraction for materials commonly used in cryogenics: (**a**) metals; (**b**) non-metals (Reprinted from Ekin [6])

2.3 Conductivities: Electrical and Thermal

The electrical and thermal conductivities are non-equilibrium transport properties that determine, among other things, the heat generated due to current flow or the heat flow due to a temperature difference. In general, the electrical and thermal conductivity of pure metals is higher than that of alloys, which is why pure copper,

aluminum and silver are common electrical conductors or thermal conduction straps in cryogenic systems. On the other hand, insulating materials and composites do not carry electrical current at all and for the most part have lower thermal conductivities, which makes such materials best for thermal and electrical insulating supports. Some special crystalline insulators have high thermal conductivities that are useful for electrical insulating connections that require good thermal contact.

2.3.1 Electrical Resistivity of Metals

Near room temperature, the electrical resistivity of most pure metals decreases monotonically with temperature following an approximately linear relationship. This trend is the result of electron–phonon scattering and is the dominant temperature-dependent contribution to the resistivity $\rho(T)$. At low temperatures, the resistivity trends to a constant value, which is approached when the metal is near liquid helium temperature. The constant value of low temperature is referred to as the residual resistivity ρ_0 and is strongly dependent on the purity and amount and distribution of lattice imperfections in the metal. Generally, these two effects are additive, obeying what is known as Matthiessen's rule that the total resistivity is the sum of two contributions,

$$\rho = \rho_0 + \rho(T) \tag{2.20}$$

As an example of the behavior of electrical resistivity consider Fig. 2.6, which is a plot of $\rho(T)$ for various purities of copper, defined in terms of the residual resistivity ratio [RRR $= \rho(273\ \text{K})/\rho\ (4.2\ \text{K})$]. The more pure and defect free the metal, the higher its RRR value. It should also be noted that the temperature at which essentially constant resistivity is obtained decreases with increasing purity. The other point of interest in the figure is that the high-temperature ($T \approx 300$ K) resistivity is essentially independent of RRR, consistent with the dominance of electron–phonon scattering. This universal form for the resistivity of pure metals makes them very useful as temperature sensors. For example, platinum resistance thermometers are often preferred for accurate measurements in the intermediate temperature regime (30–300 K) where their sensitivity, dR/dT, is roughly constant. The electrical resistivity is one of the easiest properties to measure and as a result $\rho(T)$ is known and tabulated for many elements and alloys of interest [13–18].

The theoretical interpretation of electrical conductivity of metals associates the loss mechanism with scattering processes between the electrons and the lattice. Considering a low-frequency transport of electrical current in a metal, we can relate the conductivity to the mean scattering time, $\tau \approx l/v_F$, where l is the mean free path between electron scattering events and $v_F = (2E_f/m)^{1/2}$ is the Fermi velocity. Elementary theory of electrical conductivity gives σ as,

$$\sigma = \frac{ne^2\tau}{m_e} \tag{2.21}$$

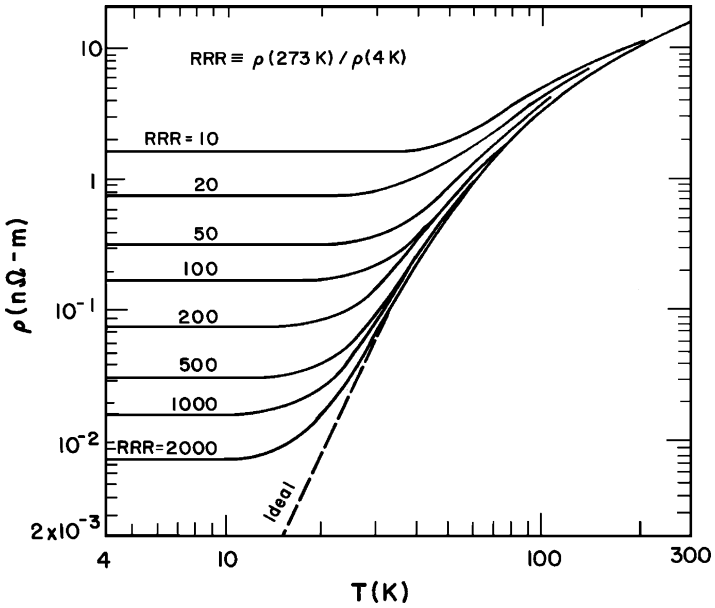

Fig. 2.6 Electrical resistivity versus temperature of differing purities of copper, $\rho(273\ \mathrm{K}) = 15.45\mathrm{n}\Omega\ \mathrm{m}$ (Reprinted from Powell and Fickett [13])

where $n = N_e/V$ is the number of conduction electrons per unit volume and m_e is the electron mass.

As mentioned above, there are two principal types of electron-lattice scattering that determine the magnitude of the electrical conductivity. For fairly high temperatures, $T \approx \Theta_D$, the dominant mechanism is due to electron scattering by quantized lattice vibrations, phonons. A simple way to see the temperature dependence of this effect is to relate the magnitude of the phonon scattering with the mean square displacement of the molecules in the lattice, $<x^2>$. In a simple harmonic solid, this quantity is proportional to $k_B T$, the thermal energy of the lattice. Assuming that the electrical resistivity is proportional to the magnitude of phonon scattering, near room temperature the resistivity of metals should also be proportional to T, a fact borne out at least approximately by the data.

For low temperatures, $T << \Theta_D$, the phonon scattering decreases with T giving way to scattering dominated by lattice imperfections. In this domain the resistivity approaches a temperature-independent value determined primarily by the amount of impurities and imperfections in the lattice. For metallic elements, a few parts per million of impurities can have a profound effect on electron transport as can the amount of cold work generated imperfections. At the lowest temperatures with the purest samples, the mean free path of the electrons can become very large approaching the sample size, such that scattering off the surface of the sample can contribute a size effect dependence to the resistivity.

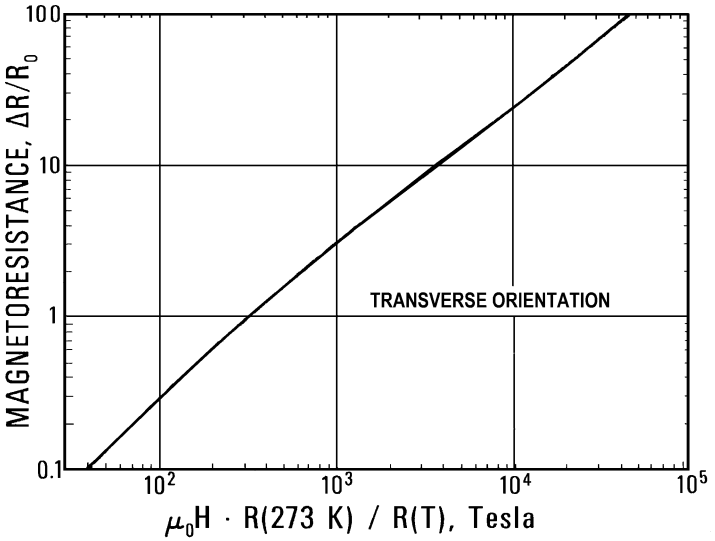

Fig. 2.7 Kohler plot for magneto-resistance of copper (Reprinted from Fickett [19])

At intermediate temperatures, $T \approx \Theta_D/3$, the resistivity varies smoothly between the two regions. Many metals have a roughly T^5 dependence in this regime which can be attributed to the phonon population being proportional to T^3 and the probability of scattering through large angle having a T^2 dependence. The resistivity is therefore proportional to the product of these two factors.

2.3.2 Magneto-Resistance in Metals

The electrical resistivity of pure metals generally increases with applied magnetic field. This effect is most significant for pure metals at low temperatures because of their relatively long mean free paths for electron scattering. Physically, magneto-resistance comes about from the fact that the electrons in the metal are deflected from a straight path in the presences of an applied magnetic field. Since the deflected path will have a greater opportunity for the electrons to scatter, the electrical resistivity would be expected to increase monotonically with applied magnetic field. The magnitude of the effect depends on the type of metal, its purity and the magnitude and orientation of the applied magnetic field.

No simple theory is available for calculating the magneto-resistance of a particular metal. However, a considerable amount of data exists and correlations are available for calculating the magnitude of the effect in common metals. For copper, the magneto-resistance is often tabulated in terms of what is known as a Kohler plot [19], shown in Fig. 2.7. To utilize this plot one needs to know the RRR = $\rho(273\ \text{K})/\rho\ (4.2\ \text{K})$ of the copper sample, the applied magnetic field ($\mu_0 H$), in this case transverse to the axis of the sample, and the desired operating temperature.

Table 2.4 Electrical resistivity of various technical alloys (units of nΩ-m) [3, 14]

Alloy	10 K	20 K	50 K	100 K	200 K	300 K	RRR
AL 5083	30.3	30.3	31.3	35.5	47.9	59.2	1.95
AL 6061-T6	13.8	13.9	14.8	18.8	30.9	41.9	3
304 SUS	490	491	505	545	640	720	1.46
BeCu	56.2	57	58.9	63	72	83	1.48
Manganin	419	425	437	451	469	476	1.13
Constantan	461	461	461	467	480	491	1.07
Ti-6%Al-4%V	1,470	1,470	1,480	1,520	1,620	1,690	1.15
PbSn (56-44)	4.0	5.2	16.8	43.1	95.5	148	37
Pt	–	0.367	7.35	28	69.2	107	290

From this information, one can calculate the magneto-resistance contribution to the total value of RRR, which in turn allows determination of the effective resistivity of the metal. However, it is important to keep in mind that this is an approximate correlation and only suitable for copper. By contrast, magneto-resistance measurements on pure aluminum do not yield a similar universal correlation. In general, the magneto-resistance makes the largest contribution to the resistivity at high field and low temperatures for pure metals.

Example 2.2

For an applied magnetic field of $\mu_0 H = 10$ T, calculate the effective RRR for a sample of copper, which has a RRR = 100 at $\mu_0 H = 0$.

In this example, the product, $\mu_0 H \times RRR = 1{,}000$ T. Using the Kohler plot for transverse magnetic field, Fig. 2.7, the magneto-resistance contribution can be estimated to be $\Delta R/R_0 \approx 3$. This value must be added to the resistance of the metal at zero field, which makes the ratio $R_{10}/R_0 \approx 4$. Thus, the sample has approximately the same electrical resistivity as a RRR = 25 sample on zero background field. The resistivity of copper at 273 K is 15.6 nΩ-m [3]. This means that the resistivity of the copper at liquid helium temperature and $B = 10$ T should be $\rho \sim 0.62$ nΩ-m, which compares reasonably well with tabulated data, which gives a value of 0.56 nΩ-m for these conditions.

The electrical resistivity of metallic alloys is generally higher than that of corresponding pure metals. Also, the temperature dependence of the resistivity of alloys is much weaker. Mostly these effects are due to the large amount of lattice imperfection scattering that occurs in concentrated alloys. The electrical resistivity of a variety of metallic alloys is given in Table 2.4. Note that the RRR for most of these metals, which varies from approximately unity for Constantan (Cu57% Ni43%) and Manganin (Cu84%Mn12%Ni4%) to 2 or 3 for aluminum alloys and over 30 for PbSn solder is considerably smaller than that of pure metals. Also, the room temperature resistivity can be very high up to two orders of magnitude greater than that of pure metals. Both of these features make alloy metals particularly useful for heaters and instrumentation leads in cryogenic applications.

2.3.3 Electrical Conductivity of Semiconductors

Semiconductors have electrical resistivities that typically range from 10^{-4} to 10^{7} Ω-m, which is many orders of magnitude higher than that of most metals ($\rho \sim 10^{-8}$ Ω-m). However, in the case of semiconductors, the low conductivity is due more to the limited number of charge carriers that exist than impurity or phonon scattering. Semiconductors possess properties that are dependent on the existence of an energy gap E_g in the electron density of states. Unlike pure metals, which do not have an energy gap, the number of conduction electrons in a semiconductor varies exponentially with temperature roughly as,

$$N_c \sim e^{-\frac{E_g}{k_B T}} \tag{2.22}$$

This exponential dependence dominates the resistivity leading to an increasing value as the temperature decreases. Such variation can be quite strong with the resistivity increasing over several orders of magnitude between room temperature and liquid helium temperature with the exact variation depending on the details of the semiconductor.

Pure semiconductors are insulators at absolute zero because the electrons cannot be excited above the energy gap, see (2.22). To overcome this limitation, the conductivity of a semiconductor can be increased by doping it with impurities that introduce additional charge carriers. Small concentrations of impurities can change the conductivity of a semiconductor by several orders of magnitude. Due to the strong temperature dependence of their resistivity, semiconductors are most commonly encountered in cryogenic applications as temperature sensors with high negative temperature coefficients. For example, high levels of sensitivity at liquid helium temperatures can be achieved using doped germanium as a sensor.

2.3.4 Thermal Conductivity of Metals

The thermal conductivity is a material property that determines the temperature gradient across a substance in the presence of a heat flow. In all materials there are several contributions to the thermal conductivity k. For metals, the principal conduction mechanisms are electronic and lattice, with the electronic contribution being dominant for pure metals. The electronic thermal conductivity can be understood by a similar model as used for electrical conductivity.

By analogy to the process of electrical conductivity, the behavior of k can be understood in terms of a kinetic theory model for gases of electrons and phonons [20]. Such simple models work very effectively to explain the limiting behavior of the thermal conductivity. In particular, the thermal conductivity may be written,

$$k = \frac{1}{3} C v l \tag{2.23}$$

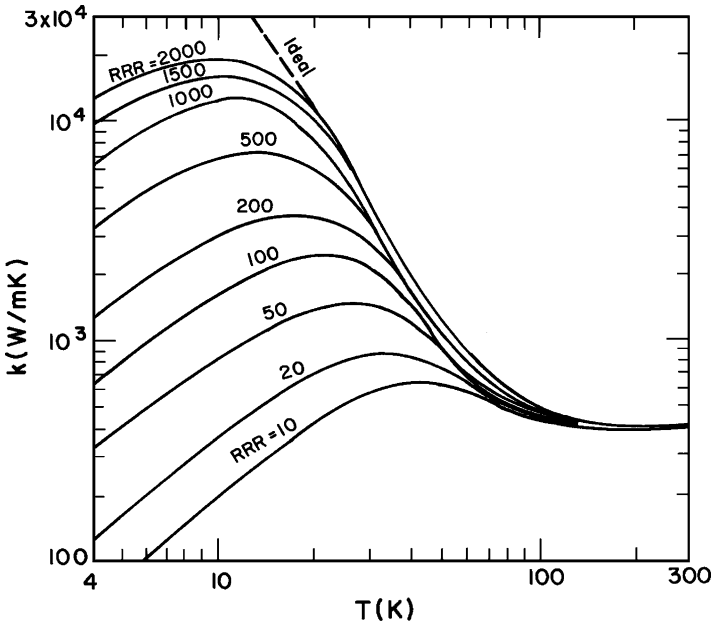

Fig. 2.8 Thermal conductivity versus temperature of differing purities of copper (Reprinted from Powell and Fickett [13])

where C is the heat capacity per unit volume, v is the characteristic speed, and l is the mean free path. Using the free-electron model, the electronic contribution to the thermal conductivity can be calculated by inserting the electronic specific heat, (2.15), and the Fermi velocity, $v_F = (2\varepsilon_F/m)^{1/2}$, into (2.23). Thus,

$$k_e = \frac{\pi^2 n k_B^2 T \tau}{3m} \tag{2.24}$$

where τ is the mean scattering time identical to that considered for electrical conductivity. At high temperatures, $T > \Theta_D$, $\tau \approx T^{-1}$ due to the increase in the lattice vibrations so that the thermal conductivity approaches a constant value. At low temperatures, τ is approximately constant, since impurity scattering dominates there, implying the thermal conductivity should be proportional to T. As an example, Fig. 2.8 shows plots of the thermal conductivities of copper analogous to Fig. 2.6 for the electrical resistivity. The limiting behavior near room temperature gives a near constant value $k = 401$ W/m K. With decreasing temperature, the thermal conductivity rises through a maximum that depends on the purity of the sample followed by a linear region ($k \sim T$) at the lowest temperatures. This system is entirely consistent with the simplified theoretical picture.

Since the electronic thermal and electrical conductivities in pure metals have similar scattering processes, a correspondence clearly should exist between these

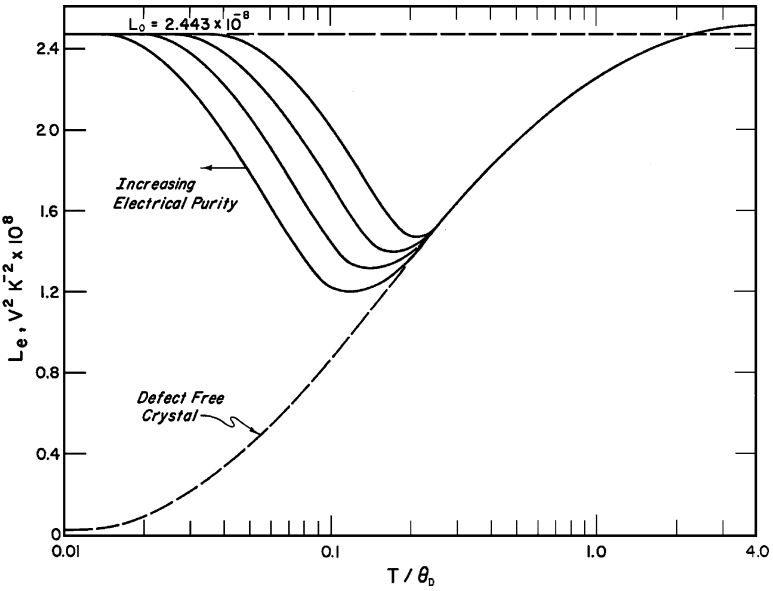

Fig. 2.9 Electronic Lorentz ratio for pure metals and defect-free metals (Reprinted from Sparks and Hurst [21])

two properties. The Wiedemann-Franz Law generally assumes that for metals the ratio of the thermal conductivity and electrical conductivity is a function of temperature only. Furthermore, for the free-electron model, this ratio is a simple expression,

$$\frac{k_e}{\sigma} = \frac{\pi^2}{3}\left(\frac{k_B}{e}\right)^2 T = L_0 T \tag{2.25}$$

where the quantity $L_0 = (\pi^2/3)(k_B/e)^2 = 2.45 \times 10^{-8}$ W Ω/K^2 is the free electron Lorenz number. L_0 is totally independent of material properties and temperature.

Experimental evidence indicates that the Wiedemann-Franz Law works only at temperatures near room temperature and at very low temperatures ($T \ll \Theta_D$) [21]. This fact is related to the asymmetry imposed on the Fermi surface when it is subjected to a thermal gradient resulting in the transport of electrons. At intermediate temperatures, the experimentally defined Lorenz ratio ($L = k/\sigma T$) is almost always less than L_0. The amount of deviation is strongly dependent on the purity of the sample, with the less pure having a smaller deviation. The overall behavior of the Lorenz ratios with sample purity are plotted in Fig. 2.9. Considerable effort has been applied to understanding these effects, the details of which are beyond the scope of the present discussion.

2.3.5 *Lattice Thermal Conductivity*

The lattice contribution to the thermal conductivity of metals, semiconductors and insulators is also understood in terms of kinetic theory although the thermal carrier in this case is a phonon gas of lattice vibrations. It is still possible to apply (2.23) although the heat capacity must be that due to the lattice, C_{ph}, which as we have discussed above is proportional to T^3 at low temperatures. Also, v is the speed of sound and l is the phonon mean free path. Most insulators and semiconductors have thermal conductivities that are several orders of magnitude lower than that of common pure metals. At high temperatures their behavior is complicated by the details of the phonon density of states, but generally the thermal conductivity decreases monotonically with temperature. At low temperatures, where scattering times become approximately independent of temperature, the thermal conductivity decreases more rapidly, approaching zero as T^n where $n \approx 3$.

The thermal conductivity of some technical materials are shown in Fig. 2.10 and listed in Table 2.5. Because the list includes a wide variety of alloys and amorphous insulators, a considerable range in values is displayed. These contain only a limited number of technically interesting materials, indicating that an area of continuing research is the determination of thermal conductivities of new materials. This need is particularly evident with the growing use of composite materials for low temperature applications.

Because the thermal conductivity of most materials used in cryogenic systems varies with temperature, it is often necessary to integrate the thermal conductivity over the temperature range of interest to obtain a total or integrated value,

$$\bar{k}(T_1, T_2) = \int_{T_1}^{T_2} k(T) dT \tag{2.26}$$

which has units of W/m. If the temperature dependence of k is known, it is straightforward to obtain $\bar{k}$ for a particular temperature range. One can then calculate the total heat flux, Q by multiplying the integrated thermal conductivity by the area to length ratio, A/L.

Example 2.3

Estimate the integrated thermal conductivity for BeCu between 1 and 300 K.

Looking at Fig. 2.10a, the thermal conductivity of BeCu is nearly linear on the log-log plot and therefore can be represented as $k \sim aT^n$, where it can be shown that $n = 1.1$ and $a = 0.4$ W/m K^{1+n} as determined from the data. It then follows that the integrated thermal conductivity is,

$$\bar{k} = \int_1^{300} aT^n dT = \frac{a}{n+1} T^{n+1} \Big|_1^{300} = 0.19\left[300^{2.1} - 1^{2.1}\right] = 30,300[W/m]$$

Note that in this case, integrated thermal conductivity is mostly determined by the upper temperature.

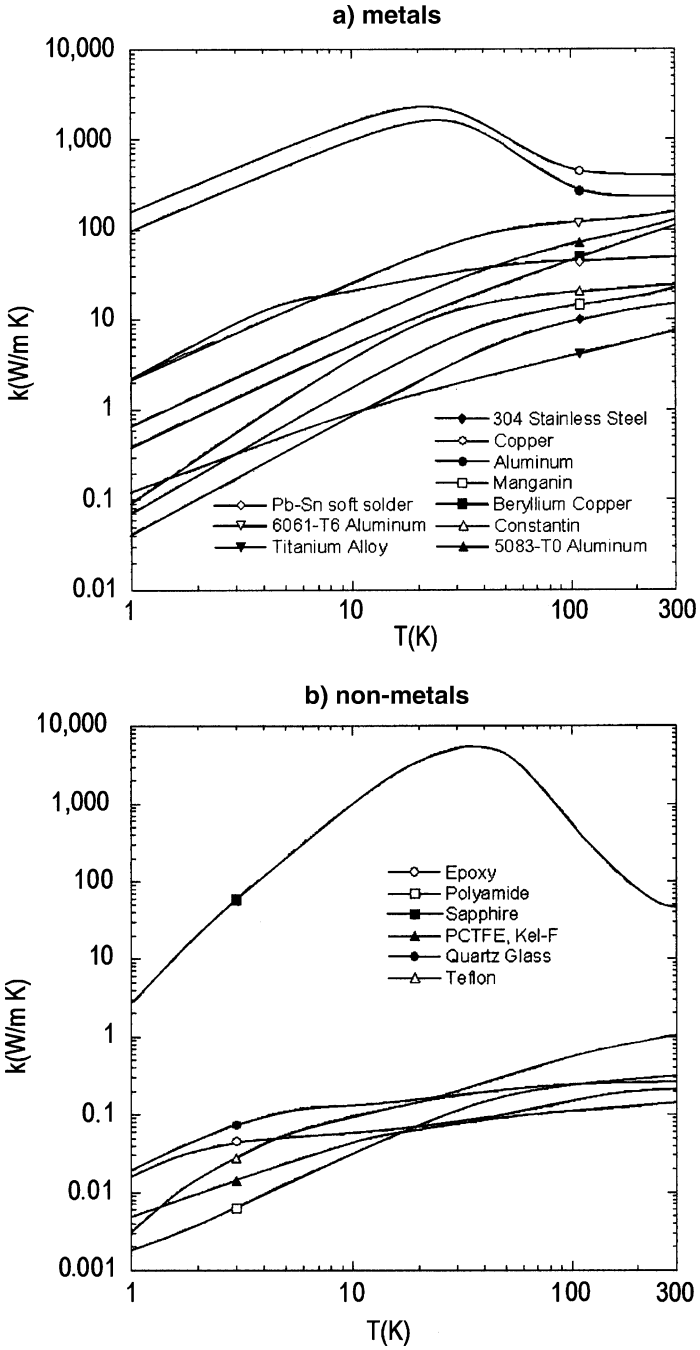

Fig. 2.10 Thermal conductivity of various materials used in cryogenics: (**a**) metals; (**b**) non-metals [3]. Symbols are used as identifiers for each material

Table 2.5 Conductivity of various technical alloys (units are W/m K) [3]

Alloy	10 K	20 K	50 K	100 K	200 K	300 K
AL 5083	30.3	30.3	31.3	35.5	47.9	59.2
AL 6061-T6	23.8	50.1	100	120	135	160
304 SUS	0.77	1.95	5.8	9.4	13	14.9
BeCu	5.1	10.3	24	44.5	79.5	112
Manganin	1.7	4.1	10.1	14	17.2	22
Constantan	3.5	8.7	18.1	20	22.8	24.9
Ti-6%Al-4%V	0.87	1.5	2.6	4	5.9	7.7
PbSn (56-44)	20	28.5	40.7	45	48	51

2.3.6 Contact Resistance

Thermal and electrical contact between materials is a topic of considerable importance in cryogenics and yet it is only qualitatively understood. Contract resistance occurring at conductor joints in magnets or other high power applications can lead to undesirable electrical losses. Poor thermal contact at the interface of a heat strap can significantly decrease the efficiency of a thermal link in a conduction cooled system. Thermal contact is also critical in the mounting of sensors for accurate temperature measurement, where failure to carefully consider this issue can lead to erroneous results. Thus, it is important to have a basic understanding of this topic for a wide variety of cryogenic system designs.

Whenever two materials are joined together for the purpose of transporting heat or electrical current a localized resistance occurs at the boundary. The magnitude of this resistance depends on a number of factors, including the properties of the bulk materials, the preparation of the interface between the two materials, whether there are bonding or interface agents present, and external factors such as the applied pressure.

The electrical contact resistance is of greatest interest in the production of joints between high purity metals such as copper, where its value can contribute or even dominate the overall resistance of an electrical circuit. Generally, the contact resistance in pure metals has a temperature dependence that scales with the properties of the bulk material, displaying among other traits a purity dependent RRR. For electrical contacts between pure metals without bonding materials like solder, the value of the electrical contact resistance decreases with applied pressure normal to the joint interface. This tendency results from an increase with pressure in the effective contact area between the two bulk samples. To understand this effect, consider that the two surfaces have microscale roughness due to how the surfaces were prepared. As the pressure is increased normal to the surfaces, the asperities tend to mechanically yield and deform increasing the effective area of contact. As the bulk material has high conductivity, the contact resistance is mostly due to the constriction of current flow that occurs at the small contact points [22]. As the contact pressure is increased, the amount of constriction for current flow decreases, thus reducing the contact resistance.

Figure 2.12 is a graphical summary of the measured electrical contact resistivity for various unbonded samples as a function of applied pressure [23]. To obtain the

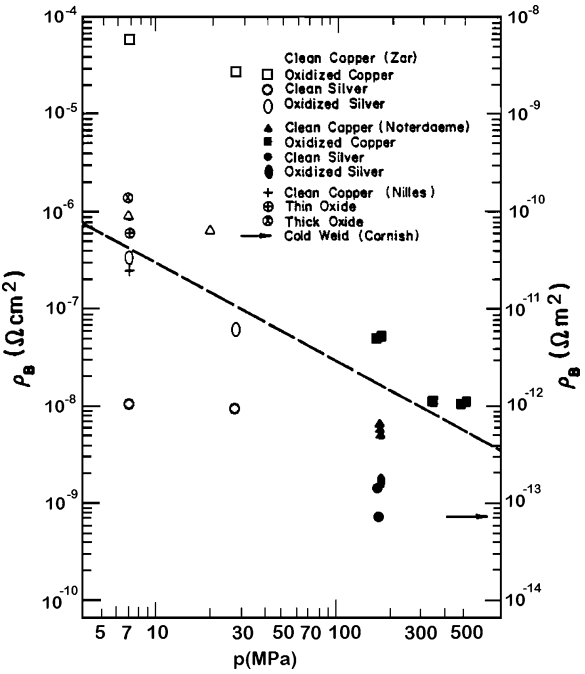

Fig. 2.11 Summary of low temperature electrical contact resistance versus pressure. *Dashed* line is the fit (2.27) [23]

contact resistance, the contact resistivity should be divided by the contact area, $R_B = \rho_B/A$. There are two things to observe in these results. First, at a particular contact pressure, there is still a wide variation in the contact resistivity, a result that is probably due to variations in sample preparation, treatment and oxidation. Second, the contact resistance generally decreases with applied pressure. The line in the graph is a rough correlation for the contact resistivity,

$$\rho_B \sim 3/p \tag{2.27}$$

where p the pressure is in Pa and ρ_B is in Ω-cm^2. This result is at least qualitatively consistent with the expected increase in area with contact pressure.

For thermal contact resistance, there are two cases to consider. First is the thermal contact resistance between metals, which would be expected correlate with the electrical contact resistance much as with bulk metals. This correlation is approximately correct for contacts between identical metals. However, if the contact is between dissimilar metals or if there are solders or other interface metals involved, the thermal contact resistance can no longer be scaled with ρ_B. This latter point is particularly significant at low temperatures where many soldiers are superconducting (Fig. 2.12).

For thermal contact resistance between non-conducting materials, the fundamental limit even for ideal contacts is the mismatch in the phonon transport across the interface [24]. Since the phonon spectra for the two materials are not the same there is an impedance mismatch that leads to a resistance occurring within roughly

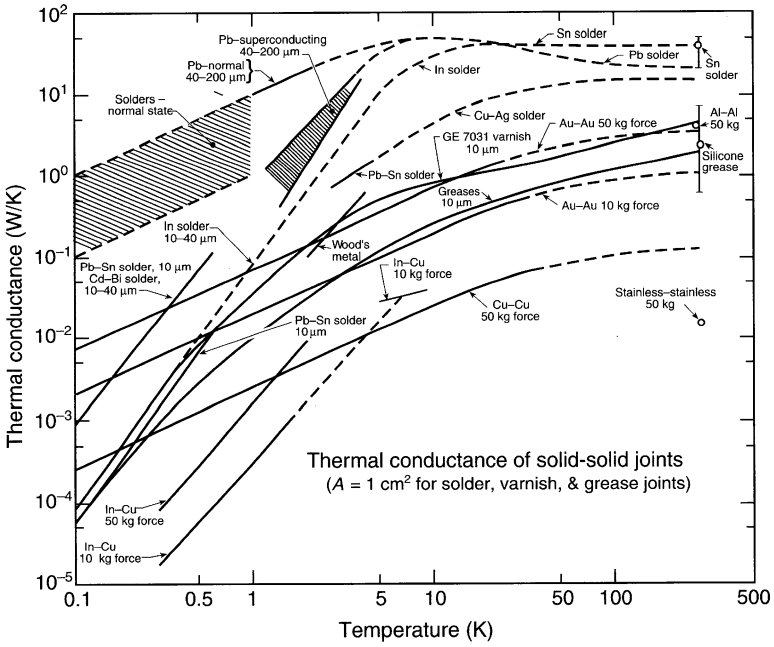

Fig. 2.12 Thermal contact conductance as a function of temperature for a variety of contact preparations and conditions. The contact assumes a 1 cm^2 area. Data compiled by Radebaugh [25] (Reprinted from Ekin [6])

one phonon wavelength of the interface. This effect is known as Kapitza conductance and is also important for heat transfer in liquid helium, a topic that will be revisited in Chap. 7. Overall, the theory of Kapitza conductance predicts a heat transfer coefficient ($h = 1/R$),

$$h_K = \left(\frac{16}{15}\frac{\pi^5 k_B^4}{h^3 c^2}\right) T^3 \tag{2.28}$$

where c is the speed of sound. Note that the speed of sound is proportional to the Debye temperature, so that low Θ_D materials would be expected to have higher thermal conductances than materials with high Debye temperature. For most solids, the factor in parentheses is on the order of 1 kW/m^2 K^4. Overall, (2.28) places an upper bound on the magnitude of the thermal contact conductance for insulating contacts. Real contacts between non-ideal surfaces are more complex and their understanding is thus more qualitative.

For joints between real materials, the interface is irregular with intermittent points of contact. In this case, the thermal contact conductance is more determined by the constriction resistance at the asperities similarly to the electrical contact resistance in metals. Thus, particularly for deformable materials without bonding agents, the thermal contact conductance should increase with interface pressure.

Experimentally, this correlation is born out with the thermal contact conductance increasing with pressure as,

$$h \approx ap^n \tag{2.29}$$

where n $\approx$ 1 and a is an empirical coefficient [23].

Thermal contact conductance varies over a wide range depending on whether the contact is insulating or conducting. Figure 2.12 displays a compilation of data for low temperature thermal contacts [25]. Some general trends can be observed. First, the thermal contact conductance values at low temperatures can range over six orders of magnitude, depending on materials and surface preparation. This large range is mostly due to variations of actual contact area and surface preparation. Second, contacts that are bonded with solder of similar agents that fill the asperities generally have higher thermal conductances than bare contacts. However, the bonding agents can also contribute to the interface resistance particularly if the bond region is thick or electrically insulating. In the low temperature region (T < 5 K), most of the data correlate with a power law, $h \sim T^n$, but there are two distinct characteristic behaviors. Pure metal-metal contacts have a temperature dependence that correlates with that of the bulk metal. Thus, at low temperature $h \approx aT$, with the coefficient of proportionality being mostly determined by sample purity and contact pressure but varying between 10^{-1} and 10^{-3} W/cm^{2}K^2. On the other hand, if the contact is bonded with solder or indium, the conductance can be much higher, but at low temperature such contacts may become superconducting. As discussed in the next section, metallic superconductors have lower thermal conductivities than in the normal state with $k_s \sim T^3$, so that the thermal conductance can in principle be reduced by introduction of bonding agents. Finally, if the interface is between two non-conducting materials, then electron transport is non-existent and the thermal conductance is generally lower following the correlation scaling with the bulk thermal conductivity, $h = aT^n$, where $n \sim 3$. However, in some special cases involving crystalline insulators, such thermal conductances can be very high as is seen with the bulk materials, see Fig. 2.10.

2.4 Mechanical Properties

The mechanical properties of materials are also very important to consider when designing cryogenic systems. Most cryogenic systems require mechanical supports to carry the loads between ambient temperature and low temperature components. Thermal transport through structural supports often significantly contribute to the overall low temperature heat load. Since the thermal conductivity of a structural material determines the heat load and the structural properties determine the required dimensions of the support, both the structural and thermal properties must be considered when designing and optimizing structural components in cryogenic systems.

The two properties that are most often of interest in a mechanical system are the stress $\sigma = F/A$ within the material and the modulus of elasticity $E_y = \sigma/\varepsilon$, where ε is the linear material strain, dx/x. These material properties enter into calculations such as mechanical deflection and failure modes in mechanical structures.

Table 2.6 Yield stress σ_y of several materials (units are MPa) [26, 27]

Material	σ_y (0 K)	σ_y (80 K)	σ_y (300 K)
304L-SS	1,350	1,300	1,150
6061-T6 Al	345	332	282
OFHC-Cu (Annealed)	90	88	75
Cu + 2 Be	752	690	552
Brass (70% Cu, 30% Zn)	506	473	420
Inconel X-750	940	905	815
G l0 – CR	758	703	414
Teflon	130	65	20

Table 2.7 Ultimate stress of several materials (units are MPa) [26, 27]

Material	σ_u (0 K)	σ_u (80 K)	σ_u (300 K)
304 L-SS	1,600	1,410	1,200
6061-T6 Al	580	422	312
OFHC Cu (annealed)	418	360	222
Cu + 2 Be	945	807	620
Brass (70% Cu, 30% Zn)	914	804	656
Inconel X-750	1,620	1,496	1,222
G-10 – CR	758	703	414
Teflon	194	86	21

Most structural materials are characterized in terms of their uniaxial stress limits. Typically, the yield stress of a material, σ_y, is defined as the load that creates a 0.2% permanent deformation; however, this definition is sometimes not meaningful particularly if one is considering a brittle material. The yield stress sometimes refers to the load that produces a distinct change in the slope of the stress–strain curve. In any case, for the design of structural components in systems, it is advisable to stay well below the specified yield stress of the material in use; typically to a maximum stress not exceeding $2/3\sigma_y$. Furthermore, in an application involving cyclic loading, this design value must be de-rated even further to take into account the failure associated with repeated application of load.

The ultimate stress σ_u, represents that level of stress necessary to cause failure of a particular material under tensile load. In ductile materials, the ultimate stress is considerably greater than σ_y and can be associated with substantial permanent deformation. On the other hand, brittle materials have $\sigma_y \simeq \sigma_u$. Composite structural materials such as fiberglass epoxy have even more complex behavior.

For most common structural materials, the yield and ultimate stresses increase with decreasing temperature. The magnitude of this increase varies from around 10% in some metallic alloys to over 100% in polymeric materials. The increase in strength is seen to result from the reduced thermal excitations within the lattice, which inhibits the spread of dislocations. Listed in Tables 2.6 and 2.7 are respectively the yield and ultimate stress values for several materials commonly used in cryogenic applications. Values listed are typical and considerable variation can occur depending on the treatment and form of the particular materials. More detailed tabulations can be found from several sources in the literature [4, 6].

Table 2.8 Young's modulus E_y of several materials (units are GPa) [26, 27]

Material	E_y (0 K)	E_y (80 K)	E_y (300 K)
304 -SS	210	214	199
6061-T6 Al	78	77	70
OFHC-Cu (annealed)	139	139	128
Cu + 2 Be	134	130	118
Brass (70% Cu, 30% Zn)	110	110	103
Inconel(X-750)	252	223	210
G-10-CR	36	34	28
Teflon	0.7	2.8	4

Table 2.9 Figure of merit (σ/k) for several different structural materials (units are MPa-m-K/W)

Material	σ/k (4 K)	σ/k (80 K)	σ/k (300 K)
304 ss	6,000	160	80
6061 T6 AL	36	3	2
G-10	12,000	1,600	500
Brass	150	9	3
Copper	2	2.5	3

The modulus of elasticity, or Young's modulus E_y, represents the change in stress level needed to cause a unit change in strain while the material is in the elastic region. Thus, Young's modulus is simply the slope of the stress–strain curve for small values of strain. As with the yield and ultimate stresses, Young's modulus also increases with decreasing temperature. A list of typical values for technical materials is shown in Table 2.8. Unlike the limiting stress values, Young's modulus is not as strongly affected by material treatment and form.

Before leaving the subject of structural materials, it is worth mentioning a method for determining the relative merits of different materials for structural applications. In the simplest example, a figure of merit (FOM) can be constructed based on the ratio of the allowable stress to the thermal conductivity (FOM $= \sigma/k$) of a particular material. Thus, high FOM materials have high strength and low thermal conductivity, such as stainless steel or certain fiberglass composites (G-10). On the other hand, a low FOM material would have high thermal conductivity and low strength, *e.g.* pure metals like aluminum and copper.

Table 2.9 shows the figure of merit for several different materials as a function of temperature. Note that the highest FOM is for G-10 composite due to its relatively high strength. On the other hand, clearly pure copper is not suitable for structural applications.

2.5 Superconductivity

Superconductivity occurs in a large number of elemental metals, alloys and now in several classes of ceramic materials. This effect, which manifests itself as an absence of electrical resistivity along with an expulsion of magnetic flux, was first observed by H. Kamerlingh Onnes in 1911 as part of an investigation of

the electrical resistance of pure metals at low temperatures. First performing such experiments with mercury, Onnes observed a sharp transition from the normal resistive state to one which had immeasurably small electrical resistance at a temperature near the normal boiling point of helium, $T \approx 4.2$ K. This new state, termed by Onnes as "supraconductive," has been the subject of much fundamental theoretical and experimental research in the many years since its discovery [28].

In the 1960s, high-field superconductive materials, mainly as Nb_3Sn and NbTi, were discovered spawning a lot of activity in high current technical applications [29]. In particular, superconductive magnets began to be developed for a wide range of applications for everything from particle accelerators to magnetic resonance imaging instruments. On a smaller scale, the high current densities in these materials made possible superconductive electronics for sensors and computers. Therefore, it is important to note that much of the interest in helium cryogenics is brought about by the existence of these materials and their applications.

Late in the 1980s, the field of superconductivity was drastically changed with the discovery of a new class of layered compounds that display superconductivity at high temperatures, near the boiling point of liquid nitrogen. Today, these materials, commonly referred to as high temperature superconductors (HTS), are actively being studied for all sorts of applications as well as for their fundamental physical properties. Their success still depends on cryogenic systems, but due to their higher operating temperatures, more effort is being placed on the development of cryogenic refrigeration in the range from 20 to 80 K. However, large scale applications of superconductivity for particle accelerators and fusion energy continue to utilize NbTi and Nb_3Sn and thus require liquid helium cryogenic systems.

In the present context, it is not possible to provide a thorough review of the physics and properties of all superconductors. For this, the reader is encouraged to seek out one of several monographs or texts on superconductivity and its applications. The present discussion, therefore, provides only a brief review of the properties of superconductors along with some discussion of their usefulness in applications.

2.5.1 Type I Superconductivity

There are two main types of superconductors with the distinction mainly associated with their electromagnetic properties. Type I superconductors, which comprise most of the pure elemental superconductors, have a sharp transition to the zero resistance state and simultaneously a total screening of magnetic flux within the bulk below T_c, the superconducting transition temperature. Thus, Type I superconductors are often referred to as perfect diamagnetic materials. The normal state in a Type I superconductor can be recovered by the application of an external magnetic field greater than the critical field H_c. Unfortunately, for Type I superconductors and their potential applications, H_c has a rather low value, $\mu_0 H_c \lesssim$ 100 mT, making Type I superconductors unsuitable for magnet and other high field applications. Type II superconductors, which sustain the superconducting state to high fields, are usable for high field applications as discussed in the next section.

Table 2.10 Critical temperature and critical field of Type I superconductors [30]

Material	T_c(K)	$\mu_0 H_0$(mT)
Aluminum	1.2	9.9
Cadmium	0.52	3.0
Gallium	1.1	5.1
Indium	3.4	27.6
Iridium	0.11	1.6
Lead	7.2	80.3
Mercury $\propto$	4.2	41.3
Mercury β	4.0	34.0
Osmium	0.7	6.3
Rhenium	1.7	20.1
Rhodium	0.0003	4.9
Ruthenium	0.5	6.6
Tantalum	4.5	83.0
Thalium	2.4	17.1
Thorium	1.4	16.2
Tin	3.7	30.6
Tungsten	0.016	0.12
Zinc	0.9	5.3
Zirconium	0.8	4.7

The magnetic field-temperature boundary between the superconducting and normal state in a Type I superconductor is given by an empirical relationship between the critical temperature and field,

$$H_c(T) = H_0\left[1 - \left(\frac{T}{T_c}\right)^2\right] \tag{2.30}$$

where H_0 is the critical field at $T = 0$ K. Listed in Table 2.10 are these parameters for known Type I superconductors [30]. Note the range of transition temperatures vary from the highest value of 7.2 K for Pb to 325 μK for Rh. A similar wide variations in the critical field is evident. It is also interesting to note that metals that are normally thought of as good conductors, copper, silver and gold, are not superconductors. This fact is related to the fundamentals of the superconducting state.

A Type I superconductor exposed to an external magnetic field $H < H_c$ will exclude the flux from penetrating into its bulk. This behavior, known as the Meissner effect, is shown schematically in Fig. 2.13. There are essentially two equivalent ways of looking at the Meissner state. The first is to note that because the superconductor has no electrical resistance, persistent screening currents are established on the surface opposing any change of the flux within the bulk. These currents flow in a layer at the surface of thickness $\lambda \approx 50$ nm, known as the London penetration depth. The London penetration depth is one of two fundamental characteristic lengths used to define the behavior of a superconductor. The alternate

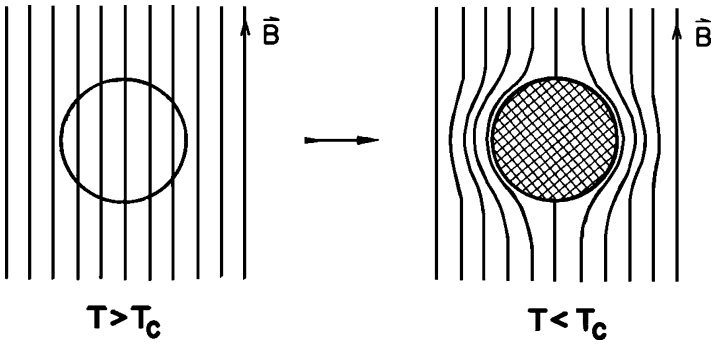

Fig. 2.13 Meissner effect in a superconducting sphere cooled in a constant applied field. Below T_c, $B = 0$ within the superconductor independent of the order of application of magnetic field and low temperature environment

picture is to consider the superconductor as if it were a perfectly diagmagnetic body such that its magnetization always equals the negative of the applied field, $M = -H$. In the superconducting state, these two interpretations lead to equivalent physics. Mainly, describing a superconductor as being a perfect diamagnet has the advantage of always predicting the flux exclusion condition independent of the order of the applied field and immersion in a low-temperature environment.

Superconductivity is brought about by the electrons in the metal forming what are known as Cooper pairs with integer spin and thus obeying Bose – Einstein statistics. This is a complex quantum mechanical phenomenon. However, one can get an appreciation for the properties of Type I superconductors that does not require advanced quantum mechanics by studying the thermodynamics of the superconducting to normal transition. In the normal state, the thermodynamic and transport properties of Type I superconductors are essentially the same as those of other normal metals and are only weakly magnetic ($M \sim 0$). On the other hand, in the superconducting state a metal is perfectly diamagnetic with $M = -H$. In follows that at the transition between the superconducting and normal states, the Gibbs free energies of the two states must be equal. The differential form for Gibbs free energy for a magnetic material is written,

$$dg = -sdT + vdp - \frac{1}{2}\mu_0 H_c^2 \tag{2.31}$$

At the critical temperature, the phase transition occurs at constant temperature and pressure so that $g_n(H_c) = g_s(H_c)$. However, since the normal state is non-magnetic $g_n(H_c) = g_n(0)$ while the superconducting state is diamagnetic, and $g_s(H_c) > g_s(0)$ by the magnetic energy density, $\frac{1}{2}\mu_0 H^2$. Thus, the difference between the Gibbs free energies at zero field may be written as,

$$g_n(0) - g_s(0) = \frac{1}{2}\mu_0 H_c^2 \tag{2.32}$$

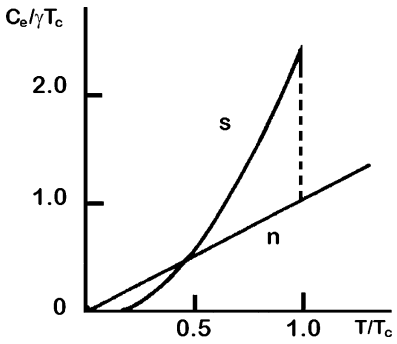

Fig. 2.14 Normalized heat capacity of superconducting and normal state of a Type I superconductor

Combining (2.32) with the empirical relationship for the temperature dependence of the critical field (2.30) yields a relationship for the entropy difference, $S_n - S_s = -\frac{\partial}{\partial T}(g_n - g_s)$ between the two states,

$$S_n - S_s = \frac{2\mu_0 H_0^2}{T_c}\left[1 - \left(\frac{T}{T_c}\right)^2\right]\frac{T}{T_c} \tag{2.33}$$

where $S = \rho s$ refers to the entropy per unit volume of the superconducting material. Note that at T_c, $\Delta S = 0$, which means that the transition is second order and there is no latent heat associated with the superconducting-normal transition at zero applied field. The heat capacity difference, $C_n - C_s = T\frac{\partial}{\partial T}(S_n - S_s)$ at the transition is obtained from the derivative of the entropy,

$$C_n - C_s = \frac{2\mu_0 H_0^2}{T_c}\left[1 - 3\left(\frac{T}{T_c}\right)^2\right]\left(\frac{T}{T_c}\right) \tag{2.34}$$

At T_c, this expression predicts a discontinuous change in the specific heat, $C_n - C_s = -4\mu_0 H_0^2/T_c$ followed by a decrease proportional to T^3 below T_c. Also, recall from Sect. 2.1.2 that the electronic contribution to the specific heat of metals dominates at low temperature, $C_e = \gamma T$. Figure 2.14 displays these dependences. Experiments have confirmed an approximately cubic temperature dependence of the specific heat for T near T_c. However, at lower temperatures, $T < 0.5\ T_c$, an exponential temperature dependence is observed. Such behavior is indicative of an energy gap in the electron density of states and is supporting evidence for the microscopic theory of superconductivity.

The behavior of thermal conductivity of Type I superconductors can be of considerable technical utility. Recall that the thermal conductivity of a metal has two primary contributions due to the transport of electrons and phonons and that it is proportional to the specific heat. For pure metals at low temperatures, the electronic contribution tends to dominate. However, in a superconductor, some of the electrons form Cooper pairs and undergo Bose-Einstein condensation into the ground state, thus being unable to carry thermal energy. As a result, the thermal

conductivity of a pure Type I superconductor is less than that of the normal state for $T < T_c$. In the vicinity of T_c, this dependence is approximately cubic in temperature dropping off exponentially at low temperatures. This behavior is consistent with the temperature dependence to the specific heat, see Fig. 2.14.

As the normal state can be restored by the application of a magnetic field greater than H_c, the thermal conductivity of a pure Type I superconductor at $T < T_c$ but $H > H_c$ should increase relative to that of the superconducting state. In particular, at low temperatures the thermal conductivity should vary linearly with temperature, $k \sim T$, consistent with the free electron model discussed in Sect. 2.3.4. Thus, the thermal conductivity of a strip of Type I superconductor below T_c can be switched by several orders of magnitude by application of an external magnetic field of greater than H_c. This operating principle is useful as a thermal switch in very low temperature refrigeration systems that cool samples to some very low temperature, $T < 1$ K. In this application, once cooled the sample can be thermally isolated by switching off the magnetic field and returning the strip to the superconducting state.

Example 2.4

A superconducting switch, consisting of a strip of tin ($T_c = 3.7$ K) surrounded by a small magnet capable of $H > H_c$, connects the cold plate of a ^{3}He refrigerator ($T = 0.5$ K) to a sample at the same temperature. Calculate the thermal conductivity ratio (k_s/k_n) assuming $k_n = \beta T$ and $k_s = \alpha e^{-(Tc/T)}$ below T_c in the superconducting state.

To find the ratio of the thermal conductivities, it is not necessary to know the absolute values. However at T_c, the thermal conductivities of the two states must be equal: $k_n(T_c) = k_s(T_c)$ or $\beta T_c = \alpha e^{-1}$. This means that $\beta/\alpha = 0.1\ \mathrm{K}^{-1}$. Note that these are not thermal conductivity units, but that is not a problem as again the goal is a dimensionless result. The important boundary condition is that the ratio β/α at T_c be unity. At 0.5 K, the ratio of the thermal conductivities is,

$$\frac{k_n(0.5K)}{k_s(0.5K)} = \frac{\beta T}{\alpha e^{-T_c/T}} = \frac{0.1K^{-1} \times 0.5K}{e^{-7.2}} = 67$$

So the switching ratio of the thermal link is nearly two orders of magnitude.

The critical current I_c is the maximum current that a superconductor can carry in the zero resistance state. This is generally a function of magnetic field. In the case of Type I superconductors, I_c is determined by the magnitude and direction of the magnetic field at the surface of the conductor as compared to H_c (Silsbee's hypothesis). In self field,

$$I_c = 2\pi a H_c \tag{2.35}$$

where a is the radius of the wire. Although H_c is relatively low, Type I superconductors can have large currents. For example, a 1 mm radius lead wire at 4.2 K in its self field can carry in excess of 260 A of resistanceless current. However, since

H_c is so low, Type I superconductors are not suitable for high field magnets. For this, fortunately we have Type II superconductors. As seen in the next section, I_c in Type II superconductors results from an entirely different mechanism having to do with the details of the microstructure.

Before leaving the subject of Type I superconductivity, it is worth mentioning a few aspects of the microscopic theory of superconductivity. The complete theory of superconductivity is based on microscopic interactions between the electrons and phonons within the lattice, leading to correlated behavior of the electrons, known as Cooper pairing. The mathematical treatment of this model is quite complex, requiring a thorough knowledge of advanced quantum mechanics, and is well beyond the scope of this brief survey. Nevertheless, there are some important results of the microscopic theory which are helpful in understanding the general behavior of superconductors.

One major success of the microscopic theory is its ability to predict the superconducting transition temperature of a metal based on knowledge of the electron and phonon energy distributions. The electron–phonon interaction which produces Cooper pairing causes a gap in the density of electron states. This gap is the origin of the exponential specific heat at low temperatures. The width of the gap is directly proportional to the superconducting transition temperature. In the microscopic theory the exact formula is derived for the critical temperature T_c,

$$T_c = 1.14\Theta_D \exp\left(\frac{-1}{UD(\varepsilon_F)}\right) \tag{2.36}$$

where Θ_D is the Debye temperature, and $D(\varepsilon_F)$ is the electron density of states a the Fermi surface. The attractive potential U is due to the electron–phonon interaction which leads to Cooper pairing of the superconducting electrons. Two interesting conclusions follow from (2.35). First, metals with high resistances near room temperature thus possessing large electron–phonon interactions and a high normal state resistivity, will also be more likely to be superconductors. This result, which is approximately borne out by experiment, explains why copper is not a superconductor. Second, metals with even numbers of valence electrons having a smaller $D(\varepsilon_F)$, since they have fewer free electrons are less likely to be superconductors. Empirically, it is found that the transition temperatures of superconductors peak with odd numbers of valence electrons in support of this theoretical conclusion [31, 32]. In its fully developed formalism, the microscopic theory of superconductivity is considered to be one of the major triumphs of theoretical solid-state physics.

2.5.2 Type II Superconductivity

Most theories of superconductivity introduce a second characteristic length, known as the coherence length, ξ. In the microscopic theory, the coherence length is roughly the size of a Cooper pair, while in macroscopic theory it represents the

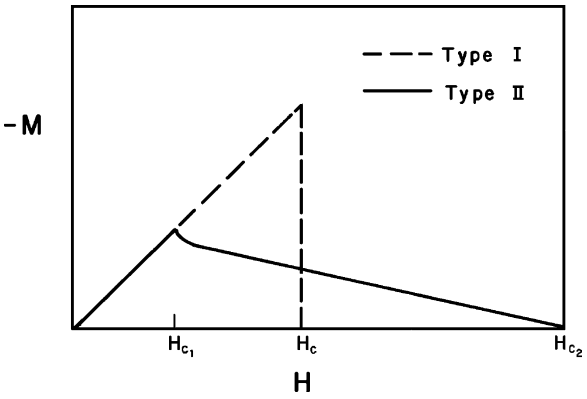

Fig. 2.15 Typical magnetization curves for metal that is either Type I or Type II superconductor. Note that for a Type II superconductor, H_c has only a thermodynamic definition

Table 2.11 Critical temperature and upper critical field of common Type II superconductors [35]

Material	T_c(K)	$\mu_0 H_{c2}$(T)
Nb	9.3	0.29
V	5.4	0.7
NbTi	9.3	13
Nb_3 Sn	18	23
V_3Ga	15	23
Nb_3 Ge	20.5	41

spatial distance over which the superconducting to normal transition occurs. The coherence length is a strong function of the crystal structure and lattice imperfections. Superconductors with large values of $\xi > \lambda$ are Type I, while Type II superconductivity occurs for those materials where $\xi < \lambda$.

The fundamental distinction between Type II and Type I superconductors can be seen by comparing their magnetic behavior. As we discussed above, in a Type I superconductor the magnetic flux is totally excluded provided $H < H_c(T)$. By comparison, in a Type II superconductor penetration of magnetic flux is allowed under certain circumstances. In an ideal Type II superconductor, the magnetic penetration is quantized in units of fluxons, $\phi_0 = h/2e$, and forms a regular triangular array, called a fluxon lattice, based on the magnitude of the external field. In effect, this brings small regions of the superconductor into the normal state. Such behavior, which is clearly a deviation from the perfectly diamagnetic Meissner state, is referred to as the mixed state in Type II superconductivity.

Because of flux penetration, the Type II superconductor in the mixed state is no longer a perfect diamagnet. A typical magnetization curve of a Type II superconductor is shown in Fig. 2.15. Also indicated is a magnetization curve for the same material if it were Type I; however in the case of Type II superconductors H_c is only defined in the thermodynamic sense and does not represent an actual magnetic transition. In Type II superconductors there are two critical fields. The lower critical field H_{c1} represents the transition from the Meissner state to the mixed state, while the upper critical field H_{c2} marks the maximum field for which any superconductivity is present. Listed in Table 2.11 are the metallic Type II superconductors that

were known prior to 1986 [32–34]. These materials are sometimes referred to as low temperature superconductors (LTS) and continue to be the materials of choice for most large superconducting magnet applications. Note that for these materials, although the critical temperature is only slightly higher than that of some Type I superconductors, H_{c2} is often orders of magnitude higher than H_c.

The mixed state in a well annealed Type II superconductor has an equilibrium condition consisting of a uniform fluxon lattice. In such a Type II superconductor, these flux lines are free to move about within the crystal. If the superconductor is subjected simultaneously to an external field and transport current, the flux lines will move under the influence of the Lorentz force, $\boldsymbol{F_L} = \boldsymbol{J} \times \boldsymbol{B}$, causing dissipation. This is an undesirable condition leading to a relatively low value of the critical current I_c. Fortunately, Type II superconductors have been developed that contain imperfections and crystal defects to pin the individual flux lines and thus restrict flux flow. Flux pinning by various forms of lattice imperfections is the dominant mechanism that allows practical superconductors to carry substantial transport currents in magnetic fields approaching H_{c2}. It is an interesting feature of superconductivity that the best properties in Type I superconductors are achieved with high purity, defect free metals while Type II superconductors performance improves by additions of impurities.

For high-field applications there are a limited number of commercially available superconductors. The two materials that are employed most often in magnets are NbTi and Nb_3Sn. NbTi is a binary alloy of approximately equal weight percent of each constituent. It has good mechanical properties, is easily processed in a composite with copper, and has a reasonably high $\mu_0 H_{c2} \approx 15$ T and $T_c \approx 10$ K. As a result, NbTi is the preferred superconductor for all magnetic devices with the exception of those requiring the highest fields, $\mu_0 H \gtrsim 10$ T. The other common practical superconductor, Nb_3Sn, is an intermetallic compound of the general class known as the A-15 s. Its mechanical properties are not as good, being very brittle, but Nb_3Sn has superior high-field characteristics, $\mu_0 H_{c2} \approx 28$ T and $T_c \simeq 18$ K, making it particularly well suited for very high-field magnetic devices. Both of these materials can be made with sufficient flux pinning to achieve high critical current densities. Also, they can be processed into multifilament wire form with copper providing a reliable product that can be cabled and wound into a wide variety of magnet designs.

Figure 2.16 shows schematically how the critical current density, J_c [A/mm^2], varies with magnetic field and temperature for NbTi and Nb_3Sn. The numerical values given in this graph are not state of the art, but rather are shown here for general trends with intrinsic variables. Also shown in the figure are the range of temperatures obtainable by the two lowest-temperature cryogenic fluids, liquid helium and liquid hydrogen. For reasonable current densities in high magnetic fields, it is apparent that low temperature helium provides the only practical coolant for these materials.

The discovery and rapid development of high temperature superconductors has introduced new opportunities for applications. This class of materials are distinct from most LTS because they are non-metals with very poor normal state conductivity. Their mechanical properties are poor and the superconducting properties are

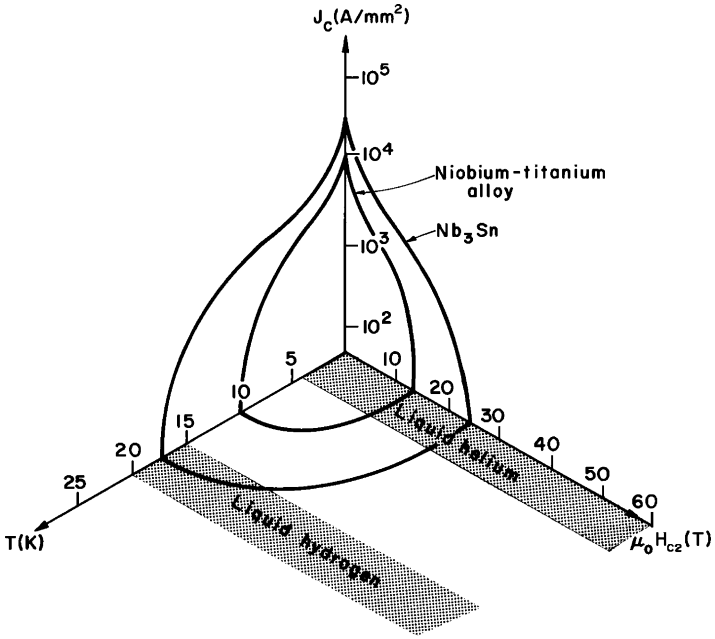

Fig. 2.16 Upper critical field, temperature, and current density for commercial superconducting materials NbTi and Nb_3Sn [35]

Table 2.12 Critical properties of HTS materials. Two values of H_{c2} indicate anisotropic material property [34]

Superconductor	T_c(K)	$\mu_0 H_{c2}$(T)
MgB_2	39	16/2.5
LaSrCuO	40	50
YBCO	90	670/120
$Bi_2Sr_2CaCu_2O_8$	90	280/32
$Bi_2Sr_2Ca_2Cu_3O_{10}$	110	
$TlBaCaCuO_{10}$	110	
$TlBaCaCuO_{10}$	125	~120
$HgBa_2Ca_2Cu_3O_8$	133	~160

more difficult to optimize due to complexities in their reaction heat treatment. Also, in most cases, these superconductors are layered structures with anisotropic properties that depend on their orientation with respect to the applied magnetic field.

Table 2.12 is a list of materials that fall broadly into the class of HTS. Note that all these materials superconducting properties are Type II. In most cases, $\mu_0 H_{c2}$ is only approximately known since its value is so high that it is difficult to measure. These materials are manufactured by different processes than LTS with the procedures being too complex to discuss in the current review. Production of HTS wire suitable for applications also depends on material selection.

Some materials, such as the BSCCO based conductors, are produced in a silver matrix, which provides the needed parallel path for electric current. Other materials such as YBCO can be formed on a variety of substrate materials.

Overall, HTS materials have transition temperatures that are sufficiently high to use other coolants such as liquid neon or nitrogen or by a closed cycle cryocooler. However, since the superconducting properties (J_c, H_{c2}) of these materials all improve with decreasing temperature, some HTS applications are still utilizing helium cooling all be it at somewhat elevated temperatures. Certainly, HTS applications have stimulated the development of small scale cryocoolers, a topic discussed in Chap. 8.

The problems of superconducting materials are of great concern to helium cryogenics. Superconducting materials require helium temperature environments to achieve their properties, but more importantly, the behavior of superconductive devices are governed largely by problems of heat transfer, efficient cooling, and safety. For example, the properties of a superconductor are conducive to carrying electric current provided the material remains below the local critical temperature and field. Thermal equilibrium is not always possible so superconductors must be fabricated in a low-resistance matrix material like copper or aluminum to provide the current-carrying capacity should the superconductor enter the normal state. Proper analysis of this problem requires knowledge of the heat transfer and fluid flow conditions present in the particular magnetic device.

Questions

1. Why does the electrical conductivity of a metal increase while that of a semiconductor decrease with decreasing temperature?
2. Why do alloys generally have lower thermal conductivity than pure metals? What does this say about material selection for structural supports in cryogenic systems?
3. Explain using thermodynamic arguments why the thermal expansion coefficient, α, of a material goes to zero as absolute zero is approached.
4. Why do materials normally get stronger as the temperature decreases?
5. Calculate the ratio σ_y/k for beryllium copper and Teflon at 300, 80 and 4 K. Compare with values in Table 2.8. Comment on their relative usefulness as structural materials.

Problems

1. Calculate the heat content in a two tonne (2,000 kg) iron magnet at 300 K. How much liquid nitrogen is required to cool this magnet to 80 K? How much liquid helium is required to cool this magnet from 80 to 4 K? (Hint: Assume that the internal energy change is entirely absorbed by the liquid resulting is a mass of vapor. Use the Debye model to calculate the change in internal energy, Θ_D(Fe) = 460 K; h_{fg}(He@ 4 K) = 21 kJ/kg; h_{fg} (N_2 @ 80 K = 200 kJ/kg)).
2. Calculate the difference between the constant pressure and constant volume heat capacities of aluminum at 300 K.

3. Derive an expression for the temperature at which the electron and phonon contributions to the heat capacity are equal. Of the elements listed in Tables 2.1 and 2.2, which has the highest value of this temperature?
4. The thermal conductivity of 304 stainless steel varies with temperature as $k(T) = 1.5\ T^{0.4}$ [W/m K]. Calculate the total conduction heat transfer for a 10 mm diameter rod, 100 mm in length. One end of the rod is at 80 K and the other is at 300 K.
5. A Pt resistance thermometer consists of a 1 m long thin wire of pure annealed platnium. Calculate the diameter of the wire based on the requirement that the power dissipation not exceed 0.1 μW at room temperature and the current be less than 10 μA. What is the sensitivity of this sensor, dR/dT?
6. Derive (2.34) starting with the Gibbs free energy change and the empirical form for the critical field of a Type I superconductor,

$$H_c = H_0\left[1 - \left(\frac{T}{T_c}\right)^2\right]$$

   a. *Adiabatic magnetization* is the constant entropy application of the magnetic field that brings the superconductor into the normal state. Derive an expression for the final temperature T_f as a function of H_0, T_c *and* T_i.
   b. Choose a Type I superconductor and calculate the value of $\Delta T_{\max}$, the maximum value for the temperature difference occurring from adiabatic magnetization.

   Hint: You may assume that the normal state specific heat $C_n = \gamma T$ and neglect the phonon heat capacity.
7. Thermal conductivity of copper

   a. Determine the mean free path in a copper sample with a residual resistivity ratio, RRR = 50 for temperatures below 10 K. Use the following values for copper: Fermi velocity $v_F = 1.57 \times 10^6$ m/s and the electron concentration $n = 8.45 \times 10^{28}\ \mathrm{m}^{-3}$.
   b. Estimate the thermal conductivity of the same copper at 2 K.

8. The maximum electrical current that can be carried by a Type I superconductor wire is limited to the current that produces the critical field H_c at the conductor surface (Silsbee's Law).

   a. Derive an expression for the critical current of a cylindrical superconducting wire of radius R as a function of temperature.
   b. How much current can a 1 mm diameter indium wire carry at 1.8 K? [Hint: Use Ampere's Law to determine the magnetic field at the surface of the wire.]

9. A normal metal wire carrying an electrical current will produce heat, raising the temperature of the wire. Estimate the time required for a copper wire carrying a current density of 100 A/mm^2 to heat up from 4.2 to 300 K if it is thermally

insulated from the environment. Assume $C_p = C_v$ and use approximations for both the resistivity and the specific heat as functions of temperature.

10. A sample of wire is made by codrawing a copper tube over an aluminum rod. The aluminum has a cross-sectional area A1 and the copper A2. The wire is stress free at ambient temperature, T = 293 K. Derive a relationship for the stress in either component of the wire as a function of A1, A2, and material properties when the wire is cooled to 4.2 K. For equal cross-sectional areas (A1 = A2), calculate the stress in the copper and compare it with the yield of annealed OFHC copper.
11. A temperature sensor located at 4.2 K requires four Manganin instrument leads to 300 K. The length of the wires is 1 m and the sensor operating current (for two of the leads) is I = 10 μA. Calculate the required wire diameter such that the thermal conduction heat load is equal to the Joule heat (I^2R) when the two leads are energized.
12. Consider a material that has a thermal conductivity varying with temperature as $k = \beta T^2$ and a constant thermal contraction coefficient, α. Derive a relationship for the overall change in length of a rod of initial length L as a function of the temperature difference between the two ends of the rod. Show the result for the special case where the low temperature end is at 0 K. Compare the answer to that for k = constant.
13. Same as Problem 12 except let the thermal conductivity be a linear function of temperature, $k = \beta T$.
14. Calculate the Lorentz ratio ($L = k\rho/T$) for one of the materials in Tables 2.4 and 2.5. Compare to the free electron value, L_0.

References

1. See for example, C. Kittel, *Introduction to Solid State Physics*, 5th ed., Wiley, New York, 1976.
2. See for example, M. W. Zemansky, *Heat and Thermodynamics*, 3rd ed., McGraw-Hill, New York, 1968.
3. CRYOCOMP® is a database code of the state and thermal properties for technical materials.
4. NIST Cryogenic Materials database: http://www.cryogenics.nist.gov/MPropsMAY/material%20properties.htm
5. G. White, *Experimental Techniques in Low Temperature Physics, 3rd Ed.*, Clarendon press, Oxford, 1979.
6. J. W. Ekin, *Experimental Techniques for Low Temperature Measurements*, Oxford University Press, Oxford, 2006.
7. K. Huang, *Statistical Mechanics*, J. Wiley & sons, NY, 1963.
8. M. Nageo, T. Inaguchi, H. Yoshimura, T. Yamada, and M. Iwamoto, Helium Liquefaction by a Gifford-McMahon Cycle Cryocooler, *Adv. Cryog. Engn.* **Vol. 35**, 1251 (1990).
9. R. J. Corruccini and J. J. Gniewek, *Thermal Expansion of Technical Solids at Low Temperatures*, NBS Monograph 29, U.S. Government Printing Office, Washington, DC, 1961.
10. T. H. K. Barron, J. G. Collins, and G. K. White, Thermal Expansion of Solids at Low Temperatures, *Adv. Phys.* **29**, 609 (1980).
11. R. S. Krishnan, R. Srinivasan, and S. Dcvanarayanan, *Thermal Expansion of Crystals*, Pergamon, Oxford, 1979.

12. G. K. White, Metals and Alloys: Expansion and Contraction, *Adv. Cryog. Engn.* **Vol. 30**, 407 (1984).
13. R. L. Powell and F. R. Fickett, *Cryogenic Properties of Copper*, International Copper Research Association, Dec. 1979.
14. R. P. Reed and A. F. Clark, *Materials at Low Temperatures*, American Society of Metals, Metals Park, Ohio, 1983.
15. L. A. Hall, *Survey of Electrical Resistivity Measurements on 16 Pure Metals in the Temperature Range 0-273 K*, NBS Technical Note 365, U.S. Government Printing Office, Washington, DC, 1968.
16. R. A. Matula, Electrical Resistivity of Cu, Au, Pd, and Ag, *J. Phys. Chem. Phys. Ref: Data* **8**, 1147 (1979).
17. G. T. Meaden, *Electrical Resistance of Metals*, Plenum Press, New York, 1965.
18. F. Clark, G. E. Childs, and G. H. Wallace, Electrical Resistivity of Some Engineering Alloys at Low Temperatures, *Cryogenics* **10**, 295 (1970).
19. F. R. Fickett, Magnetoresistivity of Copper and Aluminum at Cryogenic Temperatures, http://lss.fnal.gov/conf/C720919/p539.pdf
20. R. Berman, *Thermal Conduction in Solids*, Clarendon Press, Oxford, 1976.
21. J. G. Hust and L. L. Sparks, *Lorenz Ratios of Technically Important Metals and Alloys*, NBS Technical Note 634, U.S. Government Printing Office, Washington, DC, Feb. 1973.
22. G. K. Batchelor and R. W. O'Brien, Thermal or elecrtrical conduction through granular material, *Proc. Roy. Soc. Lon.* **A335**, 313 (1977).
23. S. W. Van Sciver, M. N. Nellis and J. Pfotenhauer, Thermal and Electrical Contact Conductance Between Metals at Low Temperatures, *Proceedings Space Cryogenics Workshop*, Berlin, Germany (1984).
24. R. E. Peterson and A. C. Anderson, Kapitza Thermal Boundary Resistance, *J. Low Temp. Phys.* **11**, 639 (1973).
25. R. Radebaugh, Thermal Conductance of Indium Solder Joints at Low Temperature, *Rev. Sci. Instrum.* **48**, 93 (1977).
26. *Handbook on Materials for Superconducting Machinery*, Metals and Ceramics Information Center, Battelle, Columbus, Pub. #MCIC-HB-04 (Jan. 1977).
27. R. F. Barron, *Cryogenic Systems*, *2nd Ed.,* Oxford Science, Oxford 1985, Ch. 2.
28. R. de Bruyn Ouboter, Superconductivity: Discoveries during the Early Years of Low Temperature Research at Leiden, *IEEE Trans. on Magnetics* **Vol. Mag-23**, 355 (1987).
29. S. W. Van Sciver and K. R. Marken, *Physics Today* **Vol. 55**, 37 (2002).
30. C. Rose-Innes and E. H. Rhoderick, *Introduction to Superconductivity*, *2nd Ed.,* International Series in Solid State Physics, **Vol. 6**, Pergamon Press, New York, 1978.
31. E. A. Lynton, *Superconductivity*, 3rd Ed., Chapman Hall Ltd. Science Paperbacks, London, 1969.
32. M. N. Wilson, *Superconducting Magnets*, Monographs on Cryogenics, Clarendon Press, Oxford, 1983.
33. Y. Iwasa, *Case Studies in Superconducting Magnets,* Plenum Press, New York, 1994,
34. J. W. Ekin, *Experimental Techniques for Low Temperature Measurements*, Oxford University Press, Oxford, 2006, Appendix A6.6.
35. B. B. Schwartz and S. Foner, Large Scale Applications of Superconductivity, *Physics Today* **30**, 34 (1977).

Further Readings

R. F. Barron, *Cryogenic Systems*, *2nd Ed.,* Oxford Science, Oxford 1985, Ch. 2
R. Berman, *Thermal Conduction in Solids*, Clarendon Press, Oxford, 1976.
J. W. Ekin, *Experimental Techniques for Low Temperature Measurements*, Oxford University Press, Oxford, 2006.
K. Huang, *Statistical Mechanics*, J. Wiley & sons, NY, 1963.

Y. Iwasa, *Case Studies in Superconducting Magnets,* Plenum Press, New York, 1994.
C. Kittel, *Introduction to Solid State Physics*, *5th Ed*., Wiley, New York, 1976.
R. S. Krishnan, R. Srinivasan, and S. Dcvanarayanan, *Thermal Expansion of Crystals*, Pergamon, Oxford, 1979.
E. A. Lynton, *Superconductivity*, *3rd Ed.,* Chapman Hall Ltd. Science Paperbacks, London, 1969.
G. T. Meaden, *Electrical Resistance of Metals*, Plenum Press, New York, 1965.
C. Rose-Innes and E. H. Rhoderick, *Introduction to Superconductivity*, *2nd Ed*., International Series in Solid State Physics, Vol. 6, Pergamon Press, New York, 1978.
M. N. Wilson, *Superconducting Magnets*, Monographs on Cryogenics, Clarendon Press, Oxford, 1983.

http://www.springer.com/978-1-4419-9978-8

Helium Cryogenics
Van Sciver, S.W.
2012, XXIV, 470 p. 220 illus., 9 illus. in color., Hardcover
ISBN: 978-1-4419-9978-8